https://doi.org/10.5194/nhess-2024-78
Preprint. Discussion started: 24 June 2024

Natural Hazards and Earth System Sciences
Discussions

Applying recession models for low-flow prediction: a comparison of regression and matching strip approaches

Michael Margreth[1,2 *], Florian Lustenberger[1 *], Dorothea Hug Peter[1], Fritz Schlunegger[2], Massimiliano Zappa[1]

[1]Mountain Hydrology and Mass Movements, Swiss Federal Institute for Forest, Snow and Landscape Research WSL, Zuercherstrasse 111, CH-8903 Birmensdorf, Switzerland
[2]Institute of Geological Sciences, University of Bern, Baltzerstrasse 1+3, CH-3012 Bern, Switzerland

[*] These authors contributed equally to this work

Correspondence to: Michael Margreth (michael.margreth@wsl.ch)

Keywords: master recession curve, low flow, recession segments, drought

Abstract. Low flows in the Swiss Plateau are expected to occur more often, to last longer and, hence, to be more severe under climate change. To predict and manage such periods of water scarcity effectively, more precise information on the drainage behavior of catchments is required. The drainage behavior of a catchment can be characterized by recession analysis methods (RAMs; e.g., recession curves) of which several have been developed in the last decades. Their recession parameters have been related to different aquifer characteristics or more general catchment characteristics like lithology, topography, or climatology. Such parameters vary widely, and the effects of uncertainties on the model's outcomes are diverse and complex. Despite the obvious potential of recession curves for prediction, they have so far not been used for operational low flow prediction and guidance for hazard mitigation. In addition, recession curves of slowly draining catchment states are hardly represented by current RAMs.

To fill the gap of RAMs representing slow draining catchment states we developed two novel RAMs, one fully automated and based on the matching strip method (MRC_slow), the other one (SDSC) relying on a careful expert-based selection of few recession segments with the slowest recession behavior. Alongside we used three established RAMs from the literature (one further matching strip model, linear regression and lower envelope in the discharge decay - discharge recession diagram). We applied the five RAMs on previously extracted low flow segments of 33 catchments in the Swiss Plateau and compared them on their recession curvatures, durations, and volumes. We designed a procedure that evaluates which of any selected RAMs best matches the recession behavior of individual low flow segments of a hydrograph. Applying this in a simulated prediction situation, we evaluated in retrospect, which of the five specifically selected RAMs predicted the low flow hydrographs between 2021 and 2022 most accurately.

We found the variability of recession durations and volumes between catchments to be higher than between the five RAMs. Within 30 of the 33 catchments, the order of recession durations and recession volumes was the same. Hence the different

https://doi.org/10.5194/nhess-2024-78
Preprint. Discussion started: 24 June 2024


Natural Hazards and Earth System Sciences
Discussions

recession behaviors of the RAMs could be related to different catchment states. Upon evaluating the low flow predictions, we found that the MRC_slow approach overall performed best followed by linear regression and SDSC. However, for operational low flow prediction we recommend using four of the five RAMs. This allows for changing the recession model(s) at every timestep if the recession behavior changes. It is also possible to present predictions with a model ensemble, indicating a range of uncertainties if several models perform similarly well. The described data-driven approach and the newly developed models are, therefore, very promising for improving low flow predictions in gauged catchments.

1 Introduction

In the last two decades the Swiss Plateau as well as the Prealps have experienced several long and severe dry periods (e.g., 2003, 2015, 2018, 2022; Fink et al., 2004; Zappa and Kan, 2007; Laaha et al., 2017; Van Lanen et al., 2016; Meusburger et al., 2022; Lustenberger et al., 2023; Brunner et al., 2019a). In general, their precipitation deficit was superimposed with heatwaves during the vegetation period, which increased the drought conditions (Brunner et al., 2019a; Hanel et al., 2018). The analysis of hydrological data resulted in the notion that the frequency of the drought occurrence has increased since 1950 (IPCC, 2023). Analyses of δ13C and δ18O isotopes of tree rings support these findings and indicate that in recent decades, droughts have not only occurred more frequently but have also been more extreme compared to the droughts during the past two millennia (Büntgen et al., 2021). Hydrological simulations, based on the Swiss climate scenarios (CH2018, 2018), indicate that in the next century the discharges of streams on the Swiss Plateau will likely decrease during summer months, which also leads to a decrease of low flows during the low flow season (Brunner et al., 2019b, c; FOEN, 2021; Muelchi et al., 2021a, b). Thus, the ecological, social, and economic impacts (Brunner and Tallaksen, 2019; Freire-González et al., 2017) of severe droughts might become more intense. To face these challenges early on and optimize water use, authorities need more precise information with a higher spatial distribution on how catchments drain during droughts. In such a context, understanding the dominant drainage behavior of a catchment under low flow conditions is crucial for predicting discharge during droughts. Such properties of a catchment can be characterized using recession curves (Tallaksen, 1995) which represents the natural decrease in discharge in the corresponding catchment. This occurs when a stream is no longer supplied with water from sources like precipitation, snow melt or artificial water return (e.g., treated wastewater or water discharged after electricity production). Various methods for analyzing such recession curves (recession analysis methods, RAMs) have been described in the literature with the aim of determining the most representative one for a catchment. Most of them are based on recession segments, which are a part of a hydrograph depicting decreasing discharge and which is extracted from continuously measured time series (see e.g., Tallaksen, 1995). There are many different approaches for conducting such an extraction (Dralle et al., 2017; Kirchner, 2009; Mendoza et al., 2003; Santos et al., 2019; Stoelzle et al., 2013; Vogel and Kroll, 1992). Some are more restrictive than others upon considering discharge data that represents the pure depletion of the catchment, which then leads to a lower number of datapoints in such a recession segment. Thus, the number of data points and their distribution vary strongly among different studies (Stoelzle et al., 2013).

https://doi.org/10.5194/nhess-2024-78
Preprint. Discussion started: 24 June 2024


Natural Hazards and Earth System Sciences Discussions

The recession behavior of a catchment can vary considerably between different individual low flow events (Carlotto and Chaffe, 2019; Posavec et al., 2006; Stoelzle et al., 2013; Tallaksen, 1995) and among seasons (Ambroise, 2016; Federer, 1973; Laaha and Blöschl, 2006; Tallaksen, 1995). In this context, a challenge in identifying a characteristic recession curve for a catchment lies in incorporating the large variability of the aforementioned dependencies and controls. Thus, there are many methods available for recession analysis, which differ in their approach and aim (see for instance the comparison by Stoelzle et al. (2013) as well as the reviews in Hall (1968) and Tallaksen (1995)). In addition, recession curves can be linked to static properties of a catchment such as the underlying lithological composition of a basin, its topography and climatological factors (Beran and Gustard, 1977; Eng et al., 2023; Knisel, 1963; Nurkholis et al., 2019; Carlier et al., 2018; Wirth et al., 2020; Floriancic et al., 2022). Most important, a holistic view on such controls offers the potential to improve a regionalization and builds the basis for predicting low flows in ungauged catchments (Laaha and Blöschl, 2006; Van Lanen et al., 2016). However, only a few methods currently exist for characterizing the slow drainage and slow- to mean-drainage behavior, highlighting the necessity for further methodological development in this direction.

Here, we explore how various RAMs could be combined for improving low flow predictions in real-time for a catchment. To this end, we developed two novel graphical approaches for identifying recession curves in 33 catchments across the Swiss Plateau. The first approach is fully automated, following the main structure of the matching strip version with an optimization algorithm. However, it considers only the lowest discharges of each recession segment. The second approach requires manual input and an additional evaluation of the data by an expert. It combines several carefully selected recession segments using different linear regressions. Only the segments representing the slowest recession behavior of the investigation period were considered. With these newly introduced RAMs, which represent slowly draining catchment states, we aimed to find those recession curves which best represent the conditions where the slow-draining storages contribute the most to low flow (e.g., porous bedrock aquifers in the Swiss Molasse basin; Wirth et al., 2020). With ongoing drainage of a catchment, the importance for discharge of these slower responding storages situated at deeper levels increases (such as groundwater aquifers with low permeability (Stoelzle et al., 2014; Bart and Hope, 2014; Reddyvaraprasad et al., 2020). We then compared the results of these two new recession models with the outcomes from employing three other recession analysis methods that were previously published in the scientific literature. This includes (i) the matching strip by Posavec et al. (2017, 2010, 2006), as well as (ii) the linear regression, and the (iii) lower envelope approaches (Brutsaert and Nieber, 1977; Stoelzle et al., 2013). We particularly evaluated volumes and duration of recession curves calculated by the different RAMs and analyzed the methodological differences between the models. We derived explanations as to how the differences in the curves of the recession models could be relied to differences in the drainage behavior of aquifers. To estimate the real-time potential of the RAMs we designed a set-up to evaluate the potential lead time (predictable time / match time) of low flow predictions that can be achieved without a priori-knowledge of ongoing low flow events (forward prediction). With that, we aim to make data-driven discharge predictions in low-flow situations based solely on RAMs. We conclude our paper with propositions on how to combine different RAMs to improve the predictions of low lows in catchments across the Swiss Plateau.

https://doi.org/10.5194/nhess-2024-78
Preprint. Discussion started: 24 June 2024


Natural Hazards and Earth System Sciences Discussions

2 Previous achievements in developing recession analysis methods (RAMs) function

2.1 Master Recession Curves (MRC) and Analytical Recession Analysis

Commonly used recession analysis methods (RAMs) can be classified into two main groups. These are approaches to identify the master recession curves (MRC) and the results of analytical recession analysis. MRCs were developed to overcome the variability of individual recession segments (Tallaksen, 1995), where MRCs are commonly identified through correlation analysis (Beran and Gustard, 1977; Langbein, 1938; Nathan and McMahon, 1990) and by the matching strip method (Snyder, 1939). Further development of both approaches focused on the reduction of user-induced biases and on the automation of the process (see e.g., Nathan and McMahon, 1990; Tallaksen, 1995; Toebes et al., 1969). In the correlation method, all discharge values (Q_y) are plotted against the discharge values with a fixed time lag z (e.g., one day; Q_{y+z}). At the perimeter of this point cloud, where the recession segments converge and intersect at the origin, an envelope is drawn (Nathan and McMahon, 1990; Beran and Gustard, 1977). The matching strip method (Carlotto and Chaffe, 2019; Lamb and Beven, 1997; Posavec et al., 2006; Snyder, 1939) aims to horizontally transpose and partially overlap several individual recession segments and create one single curve, i.e. the MRC, through the overlapping of segments. The MRC is a curve that typically results from the mean of the used recession segments and describes the average drainage properties of a catchment (Rivera-Ramirez et al., 2002). Different versions exist on how the recession segments are transposed and which mathematical functions are used to create the MRC (Ambroise, 2016; Coutagne, 1948; Fiorotto and Caroni, 2013; Posavec et al., 2017). Several authors have criticized the MRC method as being too subjective (see e.g., Smakhtin, 2001). In this context, Tallaksen (1995) recommends employing MRC methods only for an overall approximation of low flow recession at the regional scale due to the high time variability in the recession curve. Nathan and McMahon (1990) applied both methods, the matching strip method and the correlation method, to 186 catchments in Australia and found that the matching strip method was more accurate while Rivera-Ramirez (2002) found the correlation method to yield more accurate approximations of the recession behavior.

To avoid uncertainties in aligning recession segments Brutsaert and Nieber (1977) developped an analytical method to determine recession parameters by plotting the negative decline in discharge (-dQ/dt; per day) versus discharge (Q; mean per day) from recession segments on a log-log-scale. Using the slope of discharge (discharge decay per day) instead of discharge only, it is possible to eliminate the temporal dimension. Different models can be applied to this point cloud in the log-log-scale to determine the recession behavior of a catchment. Commonly, fitting has been achieved through (i) determining a linear regression to the mean (James and Thompson, 1970; Vogel and Kroll, 1992), (ii) assessing the lower envelope to the 5 % quantile (Brutsaert and Nieber, 1977) and (iii) through binning where a linear regression is fitted through binned means (Kirchner, 2009).

https://doi.org/10.5194/nhess-2024-78
Preprint. Discussion started: 24 June 2024


Natural Hazards and Earth System Sciences Discussions

2.2 Different behavior of recession models and potential for low flow prediction

The technique for extracting the recession segments and the approach to estimate the parameters of storage-outflow-models have a relevant impact on the resulting estimation of recession curves. The interaction of the impact of these two aspects is complex, which limits the comparability of recession characteristics of different catchments based on just one recession model (Stoelzle et al., 2013). The linear regression and the binning methods yield curves that describe a mean recession behavior (Stoelzle et al., 2013; Kirchner, 2009) while the lower envelope method delivers long recession times. Such information is more representative of a catchment state where contributions of slow draining reservoirs dominate the hydrograph (Brutsaert and Nieber, 1977; Stoelzle et al., 2013). To account for these differences, a combination of several methods to analyze the recession should be used at once (Rivera-Ramirez et al., 2002; Stoelzle et al., 2013).

An intriguing feature of recession models is their potential as a tool for predicting low-flow discharge. Once the discharge is close to the range of a recession curve (low flow), there is a chance that in the following days the discharge might continue to decrease at the rates predicted by this recession curve. The potential of RAMs as a simple data-informed approach for real-time discharge prediction is therefore obvious. Nonetheless, no such system has been tested for operational use by the knowledge of the authors. Also, there are few studies that effectively focus on predicting low flows based on RAMs (Singh and Griffiths, 2021; Reddyvaraprasad et al., 2020; Griffiths and McKerchar, 2015). In fact, most hydrological models are designed for mid to high flows (Staudinger et al., 2011). Among the few existing ones, Rivera-Ramirez et al. (2002) matched independently observed recession events with pre-computed models from RAMs in two basins to identify the point at which an ongoing recession segment aligns with those described by the MRC. Singh and Griffiths (2021) made a further step and analyzed the potential of MRCs to predict discharge. They found the prediction error to be acceptably small after two to three days after the start of the recession segment. Reddyvaraprasad et al. (2020) were the first to predict a recession based on coefficients that were derived from data of past discharge. Yet, it remains unclear how different RAMs (e.g., graphical, and analytical methods) compare when performing predictions.

2 Methods

2.2 Data

33 head catchments spread over the whole Swiss Plateau (Figure 1) were chosen to explore the different RAMs. Their sizes vary between 0.5 and 420 km2 and their outlet elevations range from 380 to 1000 m a.s.l (Table A1 in the Annex). For these target catchments time series of mean daily discharge values were used that were continuously measured between 1991 and 2022. The data were provided by the Federal Office for the Environment (FOEN), the Canton Aargau and the Canton Zürich. In all catchments the discharge regime is mainly pluvial (Weingartner and Aschwanden, 1992), and the underlying bedrock is characterized by different lithologies (cf. the Swiss Federal Office of Topography „Geological maps", e.g. "Lithology 500" or "Geology 500"), which potentially results in different recession behaviors.

https://doi.org/10.5194/nhess-2024-78
Preprint. Discussion started: 24 June 2024

Natural Hazards and Earth System Sciences
Discussions

As the sample size considerably affects the results of the recession analysis (Fiorotto and Caroni, 2013; Rivera-Ramirez et al., 2002), the discharge values between 1991 and 2020 were used for the fitting of the recession parameters for all catchments. The discharge values between 2021 and 2022 were used to test the prediction performance of different recession models in retrospect (see Sect. 3.7). For the development of the novel method referred to as Slow Drainage Storage curves (SDSCs), we additionally employed mean 10 min discharge values and daily rainfall sums averaged over the corresponding catchment area. The rainfall data was derived from the gridded dataset RhiresD v.2 provided by MeteoSwiss (MeteoSwiss, 2021). The discharge data of the FOEN (15 catchments) as well as the precipitation data are also openly available from the CAMELS-CH dataset (Höge et al., 2023a, b).

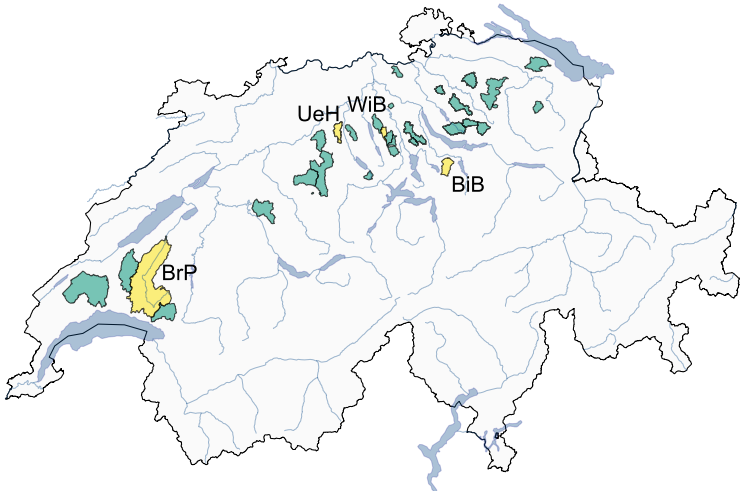

Figure 1: 33 catchments in the Swiss Plateau used in this study (green, yellow). The yellow ones are the four exemplary catchments (WiB: Wissenbach – Boswil, UeH: Uerke – Holziken, BrP: Broye – Payerne, BiB: Biber - Biberbrugg) used for illustration purposes in the results section.

3.2 Extraction of recession segments

As the extraction of the recession segment can be more important as a foundation for robust parameter fitting than the fitting method itself (Santos et al., 2019), we used the same recession segments for all models. In a first step, we extracted low flow periods from the measured daily discharge time series. For that, we developed an algorithm using the concepts of the World Meteorological Organisation (WMO; WMO, 2008). We only considered the daily discharge values between April and September to avoid the influence of snowmelt and to focus on more extreme summer droughts when the potential for evapotranspiration is highest in the Swiss Plateau (Lustenberger et al., 2022; Seneviratne et al., 2012).

In the literature, low flow thresholds are defined by the percentiles of the flow duration curve (Tallaksen, 1995), and they are typically described as an exceedance probability (see e.g. Gottschalk et al., 1997; Pushpalatha et al., 2012; Smakhtin, 2001;

https://doi.org/10.5194/nhess-2024-78
Preprint. Discussion started: 24 June 2024


Natural Hazards and Earth System Sciences Discussions

Stahl et al., 2020). We started our recession analysis at Q68 (≙ 68 % flow exceedance probability). This corresponds to a discharge value which is exceeded on average during 250 days of the year (lowest 32 % of all observed discharge values). Those segments of the recession curve that are above the more common low flow thresholds at Q70 or Q80 (Gottschalk et al., 1997; WMO, 2008) are needed as they define the shape of the upper part of the curves.

Our algorithm for finding recession segments proceeds chronologically over the time series of discharge. The procedure of generating a possible recession segment is started on day x_1 when the discharge value is below Q68. Generally, the discharge value on the following day x_{i+1} must then be equal or lower than the discharge value on day x_i. Accordingly, the end of a segment is set on the day (x_n) before the discharge is increasing again (x_{n+1}). However, to be relevant for being used as a MRC, the recession segment should consist of at least five days in a row with equal or decreasing discharge values (WMO, 2008). Yet in the low flow range, the occurrence of measurement errors is inevitable. Such biases together with the runoff response to small precipitation events, drinking water withdrawal, water return from wastewater treatment plants, and varying evapotranspiration rates (Weisman, 1977; Kirchner, 2009; Teuling et al., 2010; Krakauer and Temimi, 2011; Ambroise, 2016) can considerably affect the low flow hydrograph. For these reasons one day registering a discharge that is slightly higher than during the preceding day is also accepted upon constructing the recession curve. Accordingly, if the value on day x_{i+1} was up to 5 % higher than the value on day x_i but the value on day x_{i+2} was again lower than the value on day x_i the recession segment was continued.

As a final criterion, the last value of the recession segments must be lower than Q74. This allows to keep only those segments that come close to the low flow threshold of Q80, which we used to conduct our analysis. Missing data in segments ≤ 20 % was accepted, meaning that in the segment with a minimum length of five days a maximum of one day during which no data was available was allowed (e.g., because of a sensor error). A maximum number of days for defining one segment was not defined.

3.3 Analytical models

We applied two analytical methods. The discharge values from the defined recession segments (see Sect. 3.2) were used as a data base. Upon applying the negative slope on the curve displaying the discharge decay per day (-dQ/dt; mm d^{-2}) instead of discharge only (Q; mm d^{-1}) it is possible to eliminate the temporal dimension and avoid uncertainties upon determining the time steps of the recession time (Stoelzle et al., 2013). In this context, Brutsaert and Nieber (1977) used a power-law function to express the relationship between -dQ/dt and discharge Q:

$$-\left(\frac{dQ}{dt}\right) = aQ^b, \quad (1)$$

where a is a factor and b an exponent. Because -dQ/dt vs. Q is usually plotted in a log-log-scale equation (1) is also log transformed (see e.g., Stoelzle et al., 2013):

$$\log\left(-\frac{dQ}{dt}\right) = \log(a) + b\log(Q), \quad (2)$$

https://doi.org/10.5194/nhess-2024-78
Preprint. Discussion started: 24 June 2024


Natural Hazards and Earth System Sciences Discussions

where log(a) represents the intercept and b the slope of a linear regression (Brutsaert and Nieber, 1977; Vogel and Kroll, 1992). We used a least squares linear regression model to determine the log(a) and b values from the log-transformed dataset, and we refer to the resulting line as REG_mean in the remainder of the text. In addition, we determined the lower envelope, which corresponds to a line where 5 % of the data lies below it. According to Stoelzle et al. (2013) we used a quantile regression. In the following, we refer to the lower envelope method as REG_q05.

3.4 Master recession curves (MRCs)

As outlined in Section 2.1, the development of master recession curves (MRCs) represents a widely used approach to analyze a recession. As a typical method to determine MRCs we chose the interactive visual basic tool, which was developed by Posavec et al. (2017, 2010, 2006) for data in an EXCEL spreadsheet. The tool itself is based on the matching strip method (Posavec et al., 2006). Even though this tool allows for an in-built extraction of recession segments, which itself is tailored for applications to continuous discharge time series, we used our own recession segments as input. This allows us to better compare the various models used in this study. We refer to the model by Posavec et al. (2017) in the remainder of the text as MRC_p. Additionally, we developed a modified MRC model (MRC_slow), which is based on the matching strip method. The goal is to better characterize the behavior of a catchment during a period of slow drainage (longer recession durations) than what has typically been described in the literature. To do so, we first sorted the recession segments using their minimum discharge values as criteria, which themselves are the last elements according to the definition of a recession segment. We proceeded through transforming the dates of the segments into a relative measure on the x-axis (i.e., day 1, day 2, …). We then assigned a relative value to the last element of each segment, which we considered as the starting position on the MRC before optimization. Here, the segment with the highest minimum value (s_1) was given a value of one, the second (s_2) a value of two, and so on up to segment sn with a value of n. We then adjusted all time values within each segment according to the assigned last value.

We excluded the steep parts of the recession segments (upper parts of the segments) to keep only the flat parts, which characterize the slower drainage. To do so we determined the mean slope between consecutive data points of all recession segments and used it as a threshold. Starting from the value at the end of the segments we compared each slope to this threshold. Once the threshold was reached everything above (upper part of the segments) was excluded. If, after this reduction, a segment consisted of less than five data points, the segment was excluded from further analysis. Through the point cloud of the remaining elements of all remaining segments an exponential curve (nonlinear reservoir) was fitted, as suggested by Maillet (1905):

$$Q_t = Q_0 e^{-ct}, \quad (3)$$

where Q_t represents the discharge on day t, Q_0 the discharge on day 0 and c the recession coefficient. It originates from the Boussinesq's nonlinear differential equation and represents a baseflow recession for aquifers. It has been demonstrated to work

https://doi.org/10.5194/nhess-2024-78
Preprint. Discussion started: 24 June 2024


Natural Hazards and Earth System Sciences Discussions

well for streams with intermittent flows (Aksoy and Wittenberg, 2011), like those in the Swiss Plateau. The coefficient of determination (R2) served as an indicator for a goodness of fit. We transposed the segments horizontally on the x-axis to optimize the R2 of the model using the optim function in R (v4.1.1 - used with RStudio v2022.12.0+353). We used the "L-BFGS-B" method, a quasi-Newton method that allows to define the bounding limits (Byrd et al., 1995). These were chosen to be ±100 days of the initially assigned relative x-values. The maximum number of iterations for the optimization was set to 1000. The version with the highest R2 represents the final MRC_slow.

3.5 Slow Drainage Storage Curves (SDSC)

We also developed a model to calculate recession curves based on a subset of a few carefully selected recession segments with the slowest recession behavior. This makes the model very sensitive to even slight impacts of rainfall events on the hydrograph. Thus, parts of the recession segments wherein rainfall events obviously influenced the hydrograph were manually identified a priori and then removed by an expert. To do so we plotted the daily mean discharge of the recession segments together with 10 min- discharge values together with the sum of daily rainfall. Additionally, recession segments which, upon visual inspection, were affected by measurement artifacts were removed. As for the MRC_slow model, the resulting segments had to consist of at least five consecutive daily discharge values. We assigned relative values to the x-axis instead of dates (cf. Sect. 3.4). Then, we performed least square linear regressions on each of the remaining recession segments thereby considering the discharge values during the last day (x_n) and the discharge five days before (x_{n-5}), as well as between x_n and x_{n-6}. We continued this procedure to the first daily discharge of the segment (x_1). For each recession segment we identified the recession with the slope closest to zero, which then allowed us to identify the slowest recession part (SRP) at the end of each recession segment.

From this subset of SRPs we selected the SRP with the flattest slope between Q75 and Q80. This particular SRP was designated as the initial SRP (SRP1) and provided the starting part of the recession curve. Next, we selected a subset of additional SRPs that fulfilled two conditions: a smaller maximum discharge and an equal or flatter slope than SRP1. From this new subset we selected the SRP with the maximum discharge and designated it as SRP2. We repeated the above-described procedure to determine SRP3, SRP4, and so on, until no further SRPs were left (Figure 2a).

SRP1 was used as the initial segment of the final recession curve, which is also referred to as the Slow Drainage Storage Curve (SDSC). The position of SRP2 was defined by a linear extrapolation of the slope of SRP1. SRP2 started at the point where the discharge value of the extrapolation is equal to the maximum discharge value of SRP2. To fill the gap between the two SRPs, the linear extrapolation of SRP1 was used to define the recession curve. The location of all further SRPs were determined with this procedure (Figure 2b). If there was a gap between the end point of the last SRP and Q99, we linearly extrapolated the last SRP to Q99. Where the discharge values of two or more SRPs overlapped, only the values of the SRP with the flatter slope were considered. Accordingly, the number of discharge values characterizing the SRPs used in the final recession curve (SDSC) is often less than five (Figure 2b), even if the original SRPs consist of at least five datapoints.

https://doi.org/10.5194/nhess-2024-78
Preprint. Discussion started: 24 June 2024

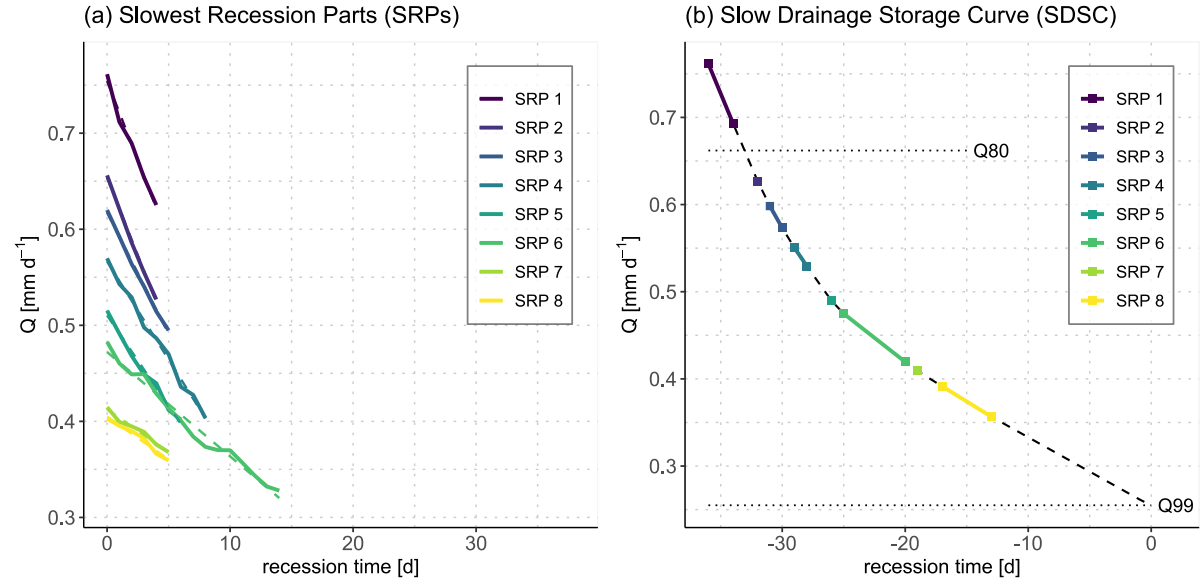

Figure 2: Illustration of (a) the eight Slowest Recession Parts (SRPs) and (b) the Slow Drainage Storage Curve (SDSC) from the same SRPs for the catchment Biber – Biberbrugg. The colored lines in (a) represent the daily mean discharge values, the dashed lines their linear regression. The colored lines in (b) represent the linear regression of the used SRPs, the dashed line the linear extrapolation and so the actual SDSC.

Only recession curves based on at least three SRPs were considered as meaningful. Additionally, in order to have a good spread of SRPs over the recession curve, the SRPs of the recession curve had to fulfill the three following criteria: (i) SRP1 must start at Q75 or higher, (ii) at least one SRP must be between Q80 and Q95, and (iii) the last SRP must end below Q95. If only two SRPs could be matched to create the SDSC or if one of the three criteria was not fulfilled, the SRPs with the flattest slopes were excluded one by one and the above-described procedure was repeated until all criteria were fulfilled.

The SDSC is the only model among the five used in this study that is not defined by a single function fitted through all points used at once. Thus, points defining a break between the linear regression parts may occur thereby pointing towards a non-linear behavior.

3.6 Visual and statistical comparison

We plotted all five RAMs (REG_mean, REG_q05, MRC_p, MRC_slow, SDSC) in the form of a recession plot (log-log plot of -dQ/dt vs. Q) and a recession curve plot (Q vs. t), respectively, to visually compare them. For the recession curve plots we horizontally shifted all models along the x-axis so that the discharge value of Q99 represents day 0 on the x-axis. We plotted the MRCs between Q80, which we defined as the low flow threshold, and Q99. Discharge values between Q99 and Q100 are assumed to be highly susceptible to measurement errors (Coxon et al., 2015; Tallaksen, 1995). Therefore, we did not use recession curve values below Q99 in our recession analysis (same as e.g., Rivera-Ramirez et al., 2002). In the recession curve plot a higher recession coefficient c (Equation (3)), pointing towards steeper curves, leads to lines that are closer to the top of

https://doi.org/10.5194/nhess-2024-78
Preprint. Discussion started: 24 June 2024


Natural Hazards and Earth System Sciences Discussions

the recession plot with the consequence that their intercept log(a) (Equation (2)) has a higher value. Accordingly, the longer the recession duration of a model the lower is the intercept log(a) in the recession plot. Slopes b = 1 represent linear reservoirs as used for e.g., the MRC_slow and MRC_p models (cf. Equation (3)). Other slopes result from the use of different mathematical equations. E.g. recession curves with steeper slopes can be characterized by a power function with the exponent 1/(2-b) as described by Kirchner (2009).

In each catchment, we calculated the specific discharge volume (volume divided by catchment area; mm) between Q80 and Q99 for all five recession models. This volume is related to the recession duration (longer recession durations generally lead to higher specific discharge volumes). We then compared the volumes of the five RAMs using the Friedman test for dependent, nonparametric samples (Friedman, 1937). We further performed Dunn's post-hoc test (Dunn, 1964) to identify statistical differences among the individual models.

3.7 Assessment of prediction performance

To evaluate the prediction performance of each model, we used the following procedure: For the independent recession segments where discharges are below Q80 a match of the discharge values to a recession curve model is made for the first element in the recession curve plot. The values of the segment on the days after the matching (between the segment and the recession curve model) may deviate. This deviation can be quantified using the corrected version of the Mean Absolute Percentage Error (MAPE), which is defined as (Makridakis, 1993):

$$MAPE_{cor} = \frac{100}{n}\sum_{t=1}^{n}\left|\frac{s_t - rc_t}{\frac{s_t + rc_t}{2}}\right|, \quad (3)$$

where rc_t is the modeled discharge of the recession curve at time step t and s_t is the recession segment at this time step. t = 1 indicates the moment when an element of the segment s matches with the values of the recession curve model. We computed the MAPEcor for three (n = 3) consecutive steps ("goodness of match range") to decide whether the match was good. If the MAPEcor of three consecutive elements of the segment was larger or equal to 5 % the matching point was disregarded, and the next element of the recession segment was evaluated. If the MAPEcor was below 5 % the corresponding point of the segment was defined as the "first match", and all successive points were then regarded as the target for the prediction by the recession curve (Figure 3a). The closer the recession segment remained to a recession curve model after the match, the more useful is the corresponding model for predicting a data-driven discharge. We used the MAPEcor calculated over all data points after the "first match" as indicator for assessing the potential for a specific recession model to predict the future discharge. We applied this procedure to all five RAMs using the recession segments from the years 2021/2022 (which were not included upon generating the recession curve models) and for all 33 catchments. We called this assessment a "forward prediction".

As a complement to the forward prediction, we calculated the agreement between a recession segment and a recession curve model, thereby starting from the last day of that segment (the day with lowest discharge: "matched point"). We did so by counting the number of days having a MAPEcor below 5 % (Figure 3b). The higher the number, the better is the agreement

https://doi.org/10.5194/nhess-2024-78
Preprint. Discussion started: 24 June 2024

Natural Hazards and Earth System Sciences
Discussions

with a specific recession model. We call this second assessment a “backward prediction». We used the Friedman test (Friedman, 1937) and the Dunn's post-hoc test (Dunn, 1964) to compare the five models in terms of their MAPEcor for the forward prediction. We considered the number of segments that could be matched for both the forward and backward predictions.

The relation between the total segment length and the predictable time/match time was analyzed using a linear regression. We used the number of predictable days as dependent variable and the available days and the RAMs as independent variables. We then calculated individual intercepts and slopes for each of the RAMs. Differences in slope and intercept for the five RAMs were assessed by the t-test of the corresponding model.

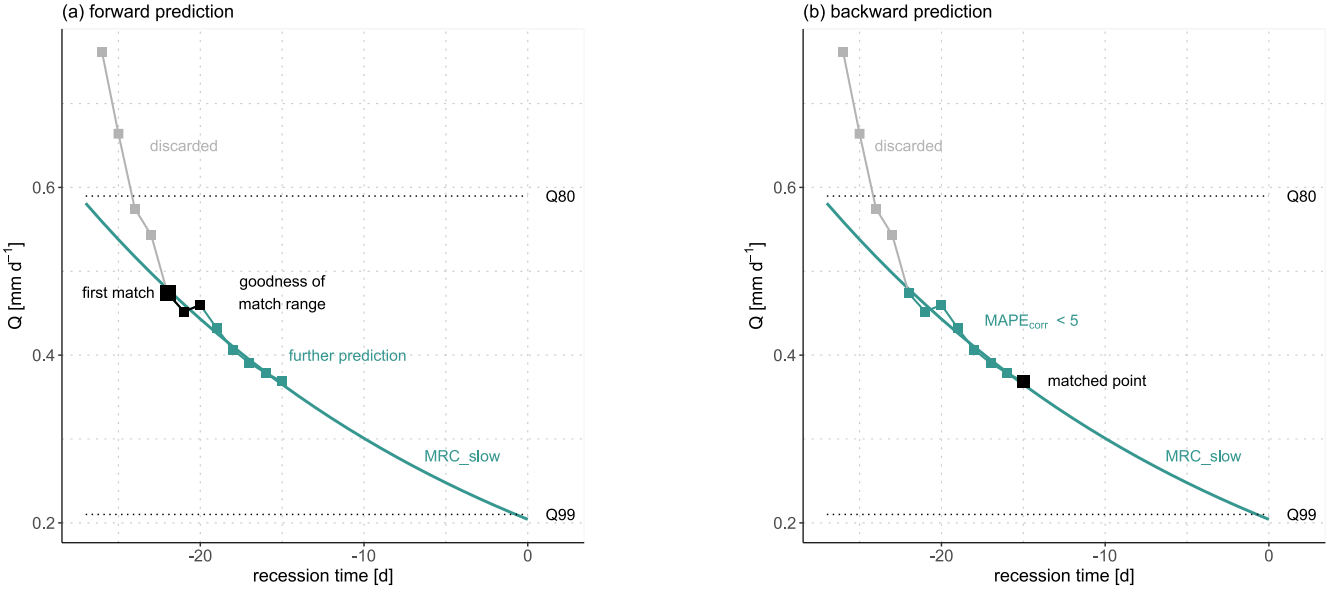

Figure 3: Visualization of the matching and evaluation procedure to assess the goodness of low-flow prediction for a recession segment in comparison to a recession model, here MRC_slow, (a) for the days between the first match and the end of the segment (forward prediction) and (b) for the days in backward direction, starting from the last element of a segment (backwards streak). The grey points represent the first elements of the segment with a poor match (MAPEcor > 5 %) with respect to the recession curve. Shown here is the example of one recession segment in the catchment Aabach in Mönchaltdorf.

4 Results

4.1 Recession duration

The recession durations from Q80 to Q99 differ considerably between the five RAMs and between the catchments. We illustrate this using four exemplary catchments (Wissenbach – Boswil (WiB), Uerke – Holziken (UeH), Broye – Payerne (BrP) and Biber – Biberbrugg (BiB); Figure 4a-d, see also Figure 1) and describe and discuss them in more detail. We justify this selection because we consider the four examples as representative for the whole dataset, mainly because they cover a large

https://doi.org/10.5194/nhess-2024-78
Preprint. Discussion started: 24 June 2024


Natural Hazards and Earth System Sciences Discussions

variety of recession durations and slopes. In all four catchments the recession durations of the five RAMs decrease in the same order: REG_q05 > SDSC > MRC_slow > REG_mean > MRC_p. However, within a catchment, the recession durations between the RAMs vary considerably. In catchment WiB and BrP the SDSC curve is rather close to the REG_q05 curve, while in catchment UeH the SDSC curve is just underneath the MRC_slow curve. In catchment WiB the curves of MRC_p and REG_mean are similar during the last 10 days of the recession, and the same is observed for MRC_p and REG_mean in catchment BiB during the last 30 days. Some recession curves have a less pronounced curvature approaching Q99 as exemplified by the recession curves in catchment UeH (with exception of the REG_mean curve). On the other hand, some have very pronounced curvatures, e.g., recession curves in catchment BiB. For the catchments WiB and BrP the curvatures of the REG_q05 curves are less pronounced than those of the other four models. For some catchments, such as catchment WiB, BrP, and BiB, the discontinuous shape of the SDSC curve is visible, indicating a non-linear drainage behavior.

For 30 of the 33 catchments, we observed the pattern of recession durations where REG_q05 > SDSC > MRC_slow > REG_mean > MRC_p (see Table A2 in the Annex). The recession durations resulting from the REG_q05 model (range: 34 to 228 days, median: 116 days) are reasonably longer than those derived from the MRC_p model (range: 10 to 23 days, median: 15 days). The SDSC model (range: 27 to 93 days, median: 52 days) returns a pattern that is approximately in the middle of the former two while the results of the MRC_slow (range: 18 to 58 days, median: 34 days) and REG_mean (range: 12 to 31 days, median: 20 days) are closer to those of the MRC_p model.

The MRC_slow and MRC_p models return curves that have a slope of 1 for all catchments (i.e., they are parallel) in the recession plot (Figure 5) but they have different intercepts. Across all 33 catchments the median intercept derived from the MRC_p model (-1.21) is higher than the one of the MRC_slow model (-1.53; cf. Figure A1 in the Annex). The REG_mean and REG_q05 models have slopes above 1 in catchments UeH and BiB but below 1 in catchments WiB and BrP. Over all 33 catchments for both models the median slopes are greater than 1 (REG_mean: 1.09, REG_q05: 1.06). The median intercept for the REG_mean model (-1.30) is higher than for the REG_q05 model (-2.04). The SDSC model yields to step-like recession plots (Figure 5). This occurs because it was created by the combination of several linear regressions (within each -dQ/dt is constant). Nonetheless, by creating a mean slope, a comparison to the other models by slope and intercept is possible. Across all 33 catchments the SDSC model has a median slope of 0.64 and a median intercept of -1.86.

https://doi.org/10.5194/nhess-2024-78
Preprint. Discussion started: 24 June 2024

Natural Hazards and Earth System Sciences
Discussions

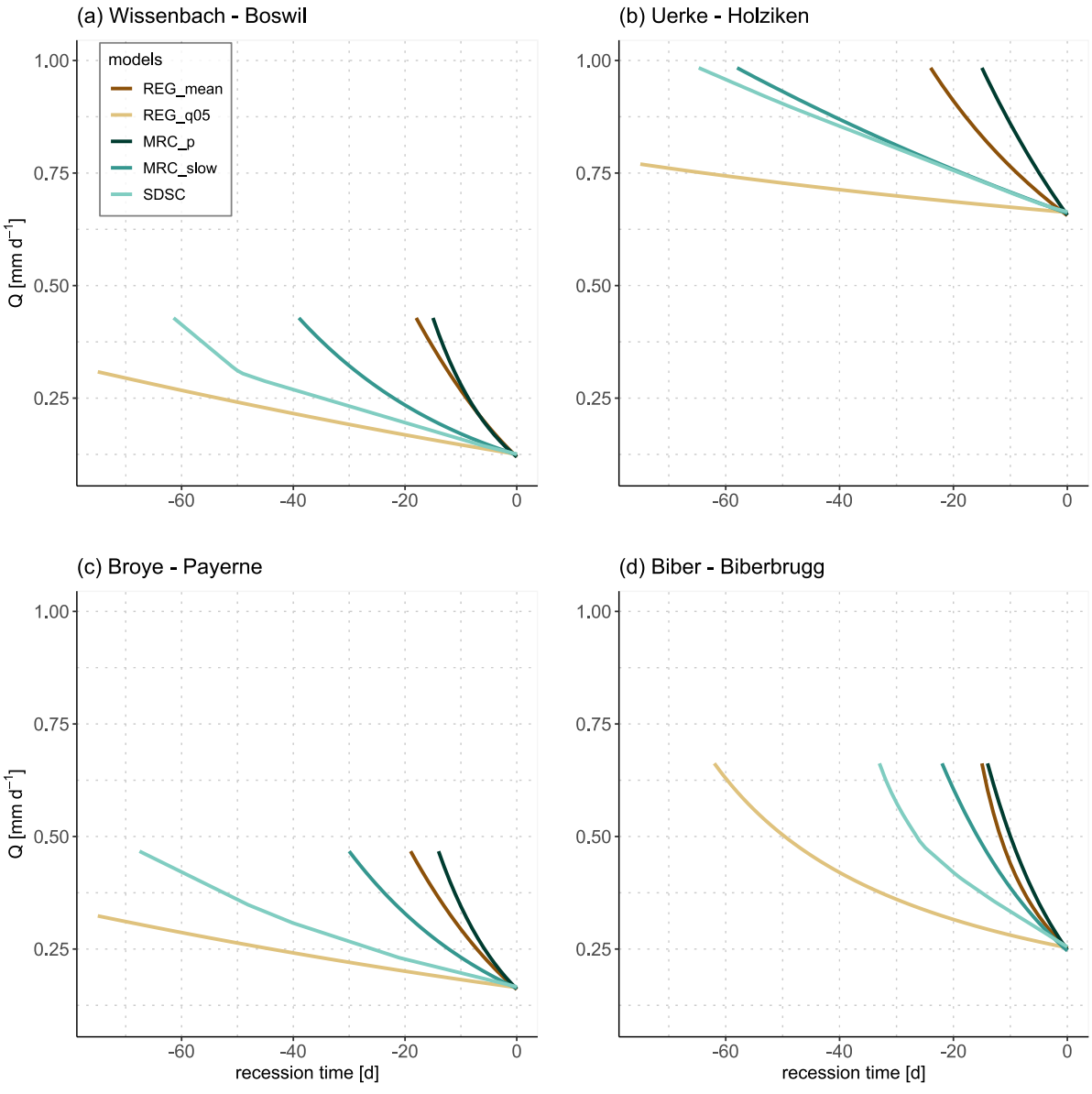

380 **Figure 4: Recession curve plots (recession time [d] vs. specific discharge [mm d-1]) with the five used RAMs (REG_mean, REG_q05, MRC_p, MRC_slow, SDSC) for four exemplary catchments in the Swiss Plateau (Wissenbach - Boswil, Biber - Biberbrugg, Ürke – Holziken, Broye – Payerne).**

https://doi.org/10.5194/nhess-2024-78
Preprint. Discussion started: 24 June 2024

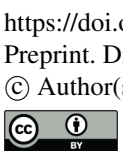

Natural Hazards and Earth System Sciences
Discussions

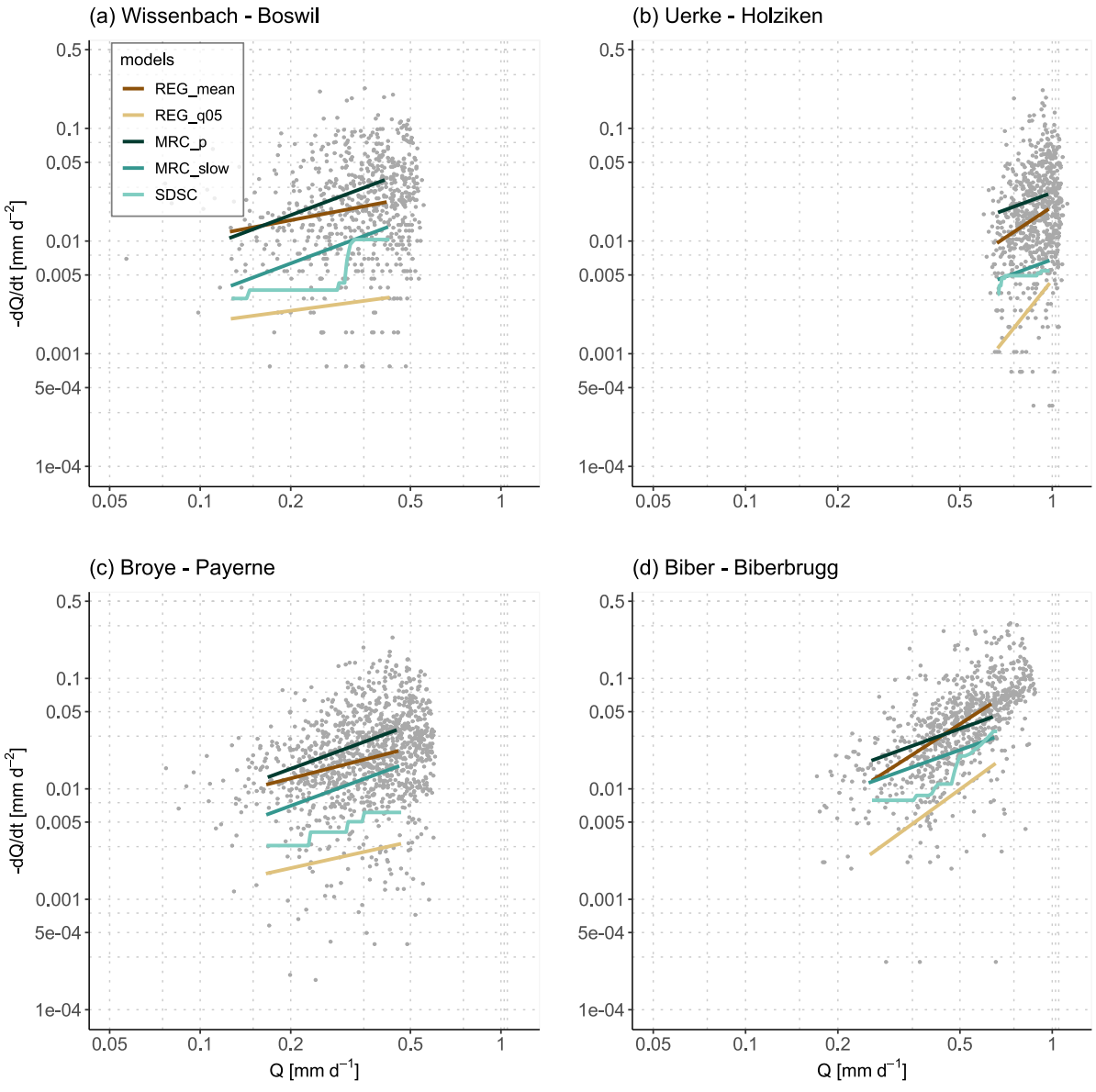

385 **Figure 5: Recession plots (specific discharge [mm d-1] vs. the negative discharge derivate after time [mm d-2]) with the five used RAMs (REG_mean, REG_q05, MRC_p, MRC_slow, SDSC) for four exemplary catchments in the Swiss Plateau (Wissenbach - Boswil, Biber - Biberbrugg, Ürke – Holziken, Broye – Payerne).**

4.2 Recession volumes

390 The REG_q05 model (range: 14.0 to 128.4 mm, median: 34.9 mm) led in most catchments to the highest recession volumes between Q80 and Q99, followed by the SDSC (range: 9.7 to 54.0 mm, median: 16.3 mm) and the MRC_slow (range: 6.2 to

https://doi.org/10.5194/nhess-2024-78
Preprint. Discussion started: 24 June 2024

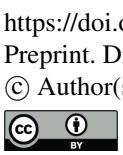

Natural Hazards and Earth System Sciences
Discussions

47.9 mm, median: 10.7 mm) models (Figure 6). The smallest volumes were retrieved by the REG_mean (range: 4.0 to 20.0 mm, median: 6.6 mm) and MRC_p (range: 3.1 to 13.0 mm, median: 5.5 mm) models, where the REG_mean model delivered a slightly greater volume than the MRC_p model. Significantly different recession volumes were found between all RAMs ($\chi 2$ = 128.17, p-value < 2.2e-16) except between REG_mean and MRC_p. Similar to the recession duration, we observed the same order for the recession volumes (REG_q05 > SDSC > MRC_slow > REG_mean > MRC_p) for 30 of the 33 catchments (Table A3 in the Annex). Note that the recession volumes between the catchments vary more compared to those of the models (see Figure 6).

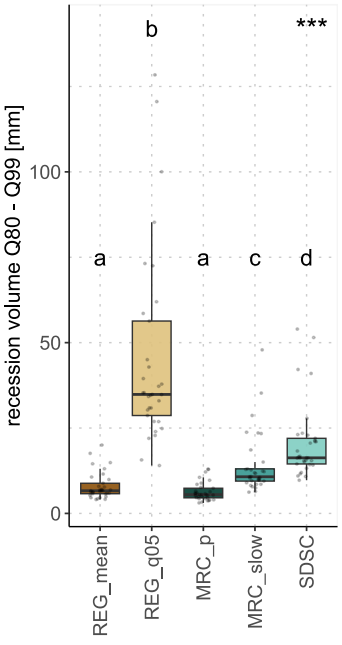

Figure 6: Boxplots of the recession volumes between Q80 and Q99 for all 33 catchments, separated for the five RAMs (REG_mean, REG_q05, MRC_p, MRC_slow, SDSC). The interquartile range (IQR; meaning the box) contains values between the 25 % and 75 % percentile, whereas the line within the box represents the median. The whiskers expand to a maximum of 1.5 times the IQR. The dots represent the actual values. Different letters denote significant differences among the models, equal letters denote no such difference. The three stars in the top right corner indicate the significance level overall (p-value < 0.001).

4.3 Forward and backward prediction

In the forward prediction, the recession segments visually matched better with the steeper RAMs (MRC_slow, REG_mean, MRC_p, SDSC) as indicated by the results of the exemplary catchment Biber – Biberbrugg (Figure 7a). The slopes of the recession segments matched better with the slopes of the models mentioned above compared to the REG_q05 model (Figure

https://doi.org/10.5194/nhess-2024-78
Preprint. Discussion started: 24 June 2024

Natural Hazards and Earth System Sciences
Discussions

7a and b). Additionally, more recession segments could successfully be matched to the recession models with steeper slopes in both the forward and backward predictions. Most of the segments were matched with the MRC_slow model (forward prediction: 8 of 9 / backward prediction: 9 of 9). The worst performance in the forward prediction was seen for the REG_q05 model, where only 3 out of 9 segments could be matched. The backward prediction was equally good for the REG_mean model but better for the other four models. For the MRC_slow and MRC_p models 9 out of 9 segments could be matched during the backward prediction.

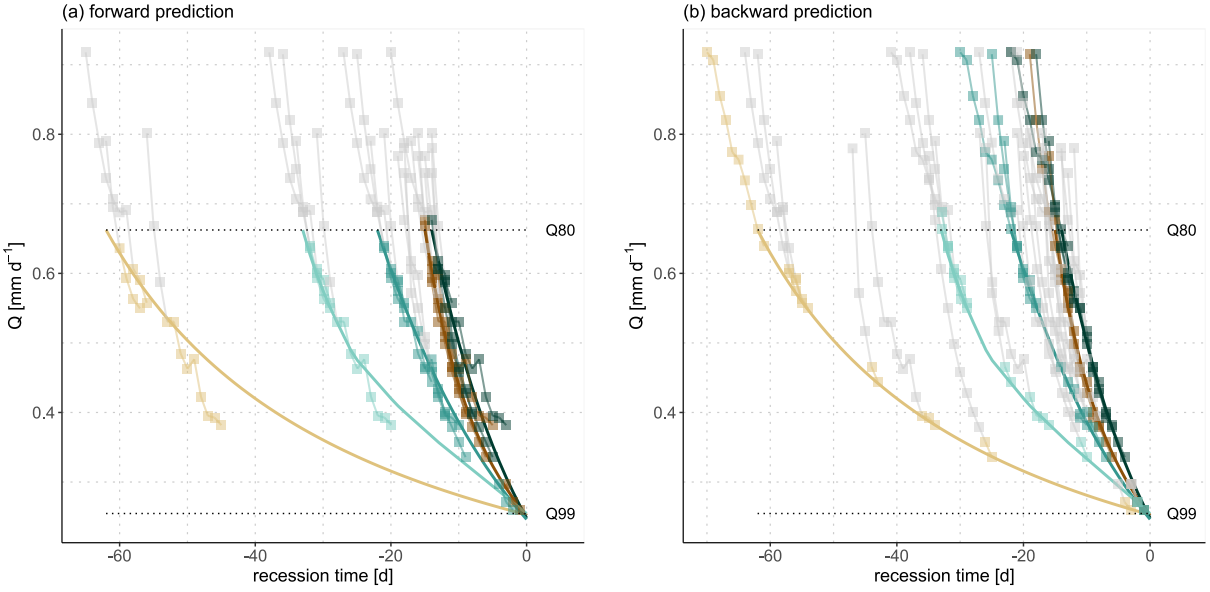

Figure 7: Recession curve plots with the five used RAMs (same colors as in the other figures) as an exemplary example of the individual recession segment matching (grey = discarded, colored = after matching) in the catchment Biber – Biberbrugg for (a) the forward prediction and (b) the backward prediction.

Table 1: Number of recession segments for the forward and backward predictions in the catchment Biber – Biberbrugg which fulfill the matching criteria with the five RAMs. The maximum number of recession segments is 9.

	REG_mean	REG_q05	MRC_p	MRC_slow	SDSC
forward prediction	6	3	4	8	4
backward prediction	6	8	9	9	8

A comparison of the forward and backward predictions of all five RAMs and for all 33 catchments reveals a similar pattern. In the forward prediction there are significant differences between the models regarding the MAPEcor ($\chi 2$ = 100.75, p-value < 2.2e-16). The lowest values, and therefore the best prediction performances, were retrieved by the MRC_slow and the REG_mean models (Figure 8, Table 2). In addition, the outcomes of both models are similar to each other. Yet slightly higher values were reached by the MRC_p model, which does not significantly differ from the REG_mean and SDSC models. The

https://doi.org/10.5194/nhess-2024-78
Preprint. Discussion started: 24 June 2024

Natural Hazards and Earth System Sciences
Discussions

highest MAPEcor values were retrieved by the REG_q05 model but it does not significantly differ from the MRC_p model. These findings correlate well with the number of segments that could be matched to the corresponding five models in all catchments (Table 2).

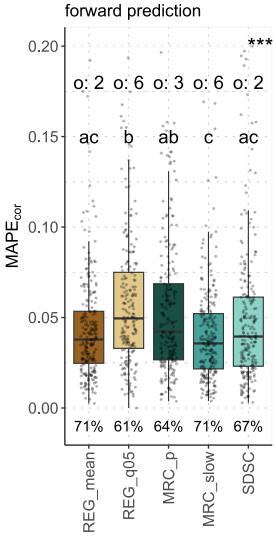

Figure 8: Boxplots showing the MAPEcor after the matching in the forward prediction for all five RAMs. The interquartile range (IQR; meaning the box) contains values between the 25 % and 75 % percentile, whereas the line within the box represents the median. The whiskers expand to a maximum of 1.5 times the IQR. The dots represent the actual values. Different letters denote significant differences among the models, equal letters denote no such difference. The three stars in the top right corner indicate the significance level overall (p-value < 0.001). The percentage values below the boxplots indicate how many segments could be matched. As the scale of the y-axis was cut, the number of points above 0.2 (n) are indicated with "o: n".

In this context, the MRC_slow and REG_mean models have the highest number (71 %), followed by the SDSC model (67 %). The worst prediction was found for the REG_q05 model (61 %). 76 of the total 336 segments could not be matched to a single model while seven could be matched to one model only. Across all models an average predictable time of 5.4 days was reached, while no large difference among the models was found (Table 2). The predictable time increases for all five RAMs with increasing segment length (Figure 9a).

In the backward prediction a slightly larger number of segments could be matched for all five RAMs (Table 2). The best model is, again, the MRC_slow (74 %), closely followed by the REG_mean (73 %). The worst performance is, again, retrieved by the REG_q05 (65 %). 51 of the total 336 segments could not be matched to a single model while 14 could only be matched to one model. Across all models an average match time of 4.0 days was reached but the models performed differently (Table 2). While the REG_q05 and MRC_p models indicated shorter match times (3.5 days), the MRC_slow model indicated higher match times (4.7 days). The REG_mean (4.0 days) and SDSC models (4.2 days) fall around the mean. In the backward prediction, the increase in match time with increasing segment length is not as pronounced as in the forward prediction (Figure 9b).

https://doi.org/10.5194/nhess-2024-78
Preprint. Discussion started: 24 June 2024

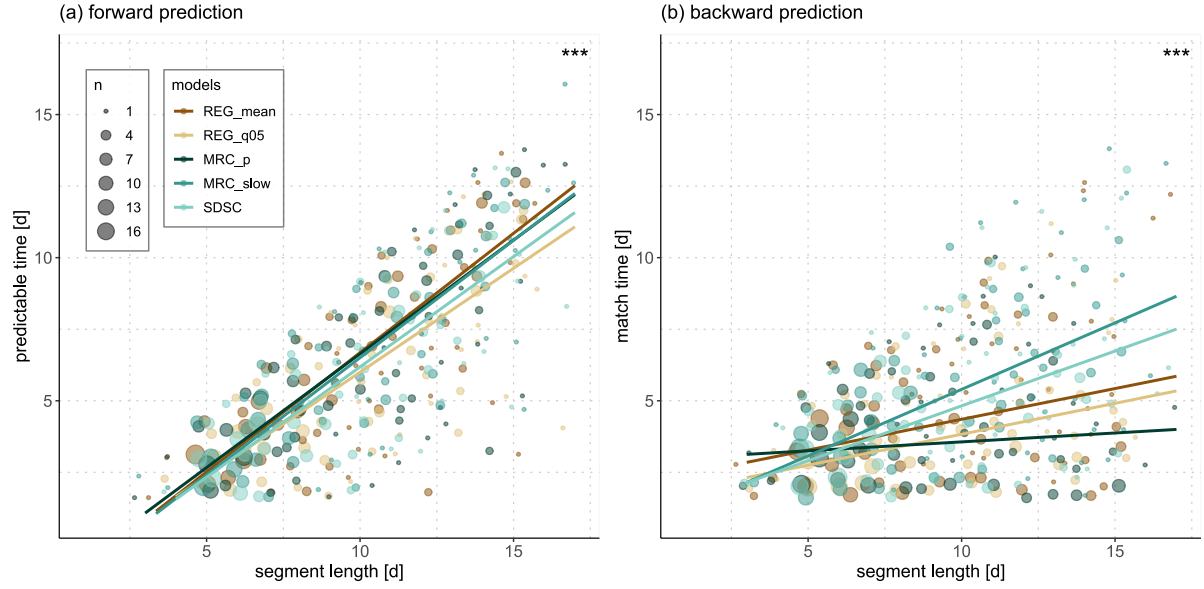

Figure 9: Dotplots for the (a) forward prediction and the (b) backward prediction, showing the recession segment lengths vs. the predictable/match time in days. The size of the points indicates how many points lie at the same location. The colors represent the five models. The lines represent linear regressions for each of the five models.

However, in this context, a larger spread between the models is found. The match time of the MRC_slow model increases the most with increasing segment length, followed by the SDSC, the REG_mean and the REG_q05 models. The MRC_p model hardly points towards an increase of the match time with segment length. In the forward prediction the linear model indicated a positive relationship between the number of predictable days and the segment length (t-value = 25.13, p-value < 2.2e-16). Only the slope of the REG_q05 model was significantly different from the REG_mean model that itself was used as reference for this calculation (t-value = -2.21, p-value = 0.03). Likewise, a positive correlation between the number of match days and the segment length was found in the backward prediction (t-value = 5.88, p-value = 5.21e-09). The MRC_slow and SDSC models had significantly different intercepts, yet the MRC_slow, SDSC and MRC_p models had different slopes compared to the REG_mean model (see Table A4 and Table A5 in the Annex).

Table 2: Percent of matchable recession segments in the forward (FP) and backward prediction (BP), the average predictable time/match time in the FP and BP as well as the average MAPEcor of the five in all 33 catchments.

model	matchable recession segments FP [%]	matchable recession segments BP [%]	average predictable time FP [d]	average match time BP [d]	average $MAPE_{cor}$ FP
REG_mean	71	73	5.5	4.0	0.046
REG_q05	61	65	5.2	3.5	0.062
MRC_p	64	71	5.6	3.5	0.056
MRC_slow	71	74	5.4	4.7	0.048
SDSC	67	71	5.2	4.2	0.052

https://doi.org/10.5194/nhess-2024-78
Preprint. Discussion started: 24 June 2024


Natural Hazards and Earth System Sciences
Discussions

5 Discussion

5.1 Recession models and catchment states

Recession durations and volumes of individual recession segments can be attributed to physical preconditions of the catchments in the beginning of a low flow period, such as saturation levels of groundwater aquifers (Ambroise, 2016; Kirchner, 2009; Tallaksen, 1995). Aquifer attributes (depth, porosity and distribution) as well as evapotranspiration (Ambroise, 2016; Kirchner, 2009; Teuling et al., 2010) impact the drainage behavior of a catchment (Tallaksen, 1995; Wang and Cai, 2010). However, despite the large differences in catchment characteristics, the order of our five models characterizing the recession durations and volumes was the same for 30 of the 33 evaluated catchments (Table 2 and table 3 in the Supplement). Similar to the diverse recession behaviors exhibited by individual recession segments, this suggests that the variances between the models can be attributed to various catchment states and characteristics. Long recession durations with flat recession curves (REG_q05, SDSC) could be an indication for a catchment state where slowly draining groundwater aquifers situated at deep levels (such as porous bedrock or highly productive Quaternary deposits, (Stoelzle et al., 2014; Wirth et al., 2020) are relatively well saturated while faster draining aquifers, such as non-productive Quaternary deposits of high permeability (like e.g., gravel sand or “Schotter”; Wirth et al., 2020) are rather empty. In addition, the losses of stored water due to evapotranspiration can be assumed to be small. On the other hand, short recession durations and steep recession curves (REG_mean, MRC_p) could indicate that storages, which generally drain quickly, are more saturated, while storages that tend to drain slowly are less saturated. Here, the losses due to evapotranspiration are likely to increase the slope of the recession curves. The MRC_slow model might often fall in-between the two described conditions and thus describes catchment conditions, which often occur during low flow periods. Accordingly, this corresponds to an average condition that is often aligned with the measured discharges (cf. low flow prediction in Sect. 5.3).

5.2 Differences between the recession models

Variations in daily discharge often disturb the storage recession in a catchment. Factors identified as the cause of these variations include uncertainties in discharge measurements, small precipitation events, anthropogenic withdrawal and return of water, or daily differences of evapotranspiration losses (Gao et al., 2022; Kirchner, 2009; Roques et al., 2017; Rupp and Selker, 2006; Stoelzle et al., 2013; Thomas et al., 2015; Westerberg and McMillan, 2015). In the literature, these variations are described as “data noise” (Laaha and Blöschl, 2006; Van Lanen et al., 2016). The five applied models differ in the way of how variations in daily discharge affect the final recession curves.

In this study, we had a particular interest in very slow recession rates, represented by the REG_q05 and SDSC models. Both models smooth the variations outlined the previous paragraph, but in different ways. For the SDSC model the previous manual filtering of the recession segments had already eliminated some of the discharge values where the measurements were biased. For the REG_q05 model such biased values are only partly eliminated by fitting the regression line (but with unfiltered recession segments) and a bias resulting in the construction of the resulting line persists (Wang and Cai, 2010). In comparison,

https://doi.org/10.5194/nhess-2024-78
Preprint. Discussion started: 24 June 2024

the REG_mean model produces considerably steeper curves compared to the REG_q05 model, resulting in smaller impacts of these unfiltered recession segments.

The SDSC model was fitted in the recession curve plot space (Q vs. t) by linear regressions within the datapoints of the same recession segments (time dependent), which partially smoothed out the impact of noise in the data. For the REG_q05 model the fitting was done in the recession plot space (-dQ/dt vs. Q) for all datapoints at once (time independent). We found that the SDSC model represents the actual recession segments more often than the REG_q05 (cf. low flow prediction in Sect. 5.3). According to Rupp and Selker (2006) the use of a constant time step (dt) for the estimation of -dQ/dt (as used for REG_q05 and REG_mean) can result in large uncertainties upon fitting the recession parameters because of noise in the data, mainly at late stages of a recession. This noise is caused by the limited resolution and precision of the measurements (Kirchner, 2009; Roques et al., 2017; Rupp and Selker, 2006) or other impacts, like short occurrences of precipitation, drinking water withdrawal, water return from wastewater treatment plants, and varying evapotranspiration rates (see Sect. 3.2). Therefore, we assume that the REG_q05 model is strongly affected by the related noise in the data.

The differences in the recession curvature, recession durations, and volumes between the SDSC model and the MRC_slow and MRC_p models can be explained by methodological differences along the models. Gaps between segments in the SDSC curves were bridged through linear interpolation, whereas for the MRC_slow and MRC_p curves, an exponential approximation was employed for model construction. In most cases the MRC_slow model produced shorter recession durations than the SDSC model. This is mainly because the MRC_slow model is based on more segments and datapoints in total, including those with small rainfall disturbances (steeper recession segments), whereas the SDSC model is based on the flattest segments. The even shorter recession durations observed in the MRC_p model are attributed to the methodological approach wherein the exponential model was fitted through the recession segments individually (from highest to lowest). In contrast, the MRC_slow model bases exclusively on the lower (flat) portion of the segments and on an optimization algorithm, which allowed to fit the MRC across all segments simultaneously.

For some catchments, the applied linear interpolation for the SDSC model leads to sharp edges or breakpoints in the resulting curve (cf. Figure 4a). Such breakpoints can naturally occur as described and/or demonstrated in several recession and baseflow studies (see e.g., Chen et al., 2012; Stoelzle et al., 2020; O'Brien et al., 2013). The SDSC relies on continuous discharge values within segments, and these breakpoints could represent:

- changes in storage depletion
- variations in evapotranspiration rates between individual recession segments
- gaps in discharge time series data within the timeframe covered by the used data for this storage state
- uncertainties in flow rating curves, which typically change multiple times within a 30-year period (personal communication with the hydrology division of the FOEN, 2024), and/or water level measurements

https://doi.org/10.5194/nhess-2024-78
Preprint. Discussion started: 24 June 2024


Natural Hazards and Earth System Sciences Discussions

Overall, among the five models utilized in this study, the SDSC model might emerge as the most reliable one for representing the slowest recession behavior observed during the 30-year examination period (April to September in catchments of Swiss Plateau). One could argue that the SDSC model represents a quasi-matching strip alternative to the REG_q05 model. However, it requires subjective manual tasks to be performed by an expert. The advantage of the other four models is that their recession curves are based on a larger number of datapoints and that they are created in a fully automated and objective way. Among these, the MRC_slow model specifically targets the average behavior of the recession segments with the slowest drainage behavior, thereby mitigating the impact of uncertainties in discharge data. Thus, of the four fully automated models, it is the one that best represents the behavior of slowly draining catchment states.

5.3 Recession models in low flow prediction

We assessed the predictive capabilities of the five models for both forward and backward predictions of discharge measurements for the years 2021 and 2022 (not used for model fitting). The prediction performance was best for both the forward and backward predictions using the two models MRC_slow and REG_mean (lowest MAPEcor values, highest percentage of matchable recession segments). This fits well to the idea where the REG_mean model represents a mean recession behavior (Stoelzle et al., 2013) and the MRC_slow characterizes a mean but rather slow recession behavior. Thus, among the five models, MRC_slow and REG_mean represent most of the recession segments. As the MRC_slow was designed for rather slower recessions it is also not surprising that it works slightly better during low flow periods. The two models representing the two extreme recession behaviors, MRC_p (mean recession; Rivera-Ramirez et al., 2002) and REG_q05 (slow recession; Stoelzle et al., 2013) are the least suitable for low flow predictions. This is reflected in the highest MAPEcor values, the smallest percentage of matchable segments, and the worst match time increase for longer segments in the backward prediction. The longer a recession period lasts, the higher becomes the contribution of slowly draining storages and hence the recession curves become flatter. Consequently, the models representing a slow catchment drainage, like MRC_slow or SDSC, are more suited compared to the other ones (highest match time with increasing segment length, Figure 9b). With longer recession segments, also longer predictable times were reached for all five models (Figure 9). Longer recession segments are typical for longer drought periods (e.g., 2003, 2018; Brunner et al., 2019c; Fink et al., 2004). As a result, better predictions can be achieved during severe dry periods than during short ones.

Some recession segments are affected by discharge fluctuations that disrupt the resulting recession curve (see Sect. 3.2 and 5.2). If such fluctuations affect the matching assessment of the forward prediction (three consecutive days from where the segments are fitted to the recession models), there might be cases where a matching is mistakenly identified. Such fluctuations could also be the reason for increasing values in MAPEcor during the forward prediction. Furthermore, some recession segments are affected by breakpoints, which could be an indication that a dominant storage ended to contribute to the hydrograph (see e.g., Chen et al., 2012; Stoelzle et al., 2020; O'Brien et al., 2013). In such situations a different recession model might be better suited to represent the ongoing recession, which can be accounted for in operational forecasting.

https://doi.org/10.5194/nhess-2024-78
Preprint. Discussion started: 24 June 2024


Natural Hazards and Earth System Sciences
Discussions

In operational forecasting, the prediction is renewed at each timestep, allowing for the exchange of models within the same interval. Performing a backwards prediction with several recession models allows the determination of the “best” performing model(s) of the past x days. The longer the match time of the backward prediction using the selected model, the more reliable the subsequent prediction may be (operational forward prediction). The "best" model, determined through backward prediction, can be employed for operational forward prediction as it accurately represents the current catchment state. However, it is also valuable to use several models at once (Stoelzle et al., 2013). If several models are similarly good performing in the backwards prediction, the model ensemble can be used for defining a confidence interval for constraining the variations in the states of catchment storage or different evapotranspiration and for assessing the uncertainties of the model (Roques et al., 2017).

Differences of the recession behavior among catchments are explained by lithological structures (Stoelzle et al., 2014; Carlier et al., 2018; Wirth et al., 2020) and local catchment characteristics. These are the occurrence and location of steep slopes and storages (Floriancic et al., 2022; Shaw et al., 2013) as well as climatic conditions (Jachens et al., 2020). But these characteristics are difficult to determine (Floriancic et al., 2022; Karlsen et al., 2016) and quantitative constraints are often not available (Gnann et al., 2021). Most affected from these uncertainties are predictions in ungauged catchments. Linking the recession models to specific catchment characteristics (such as lithological, topographical and climate factors) has the potential to improve low flow prediction in ungauged catchments. However, the possibility to find the recession model best representing the current catchment state among different models in gauged catchments enables considerable improvements in data-driven low flow predictions.

6 Conclusions

In this study, we compared five recession analysis methods (RAMs) that differ by their conceptual and methodological approach, their recession curvatures, durations, and volumes as well as by their prediction potential. Two of the five models (MRC_slow, SDSC) were developed specifically for this study. Both represent a slow to mean drainage behavior and fill a current gap in the literature. Two models are master recession curves (MRC_slow, MRC_p), whereby two of them are based on analytical methods of the discharge decay - discharge recession diagram (linear regression: REG_mean, lower envelope: REG_q05) and the SDSC is a “quasi matching strip version” of REG_q05. The five models differed considerably in their recession durations, recession volumes and recession curvatures within the same catchment. However, the order was the same for 30 of 33 catchments (REG_q05 > SDSC > MRC_slow > REG_mean > MRC_p) indicating that the variability between the catchments is higher than between the models. This suggests that the differences between the models can be allocated to different catchment states. Slowly draining recession models (SDSC, MRC_slow) are more likely to be representative for catchment states, where contributions from slowly draining aquifers dominate the low flow hydrograph and evapotranspiration rates might have a small impact. On the other hand, fast draining models (MRC_p, REG_mean) are considered to reflect those catchment states where contributions of fast draining aquifers are more dominant.

https://doi.org/10.5194/nhess-2024-78
Preprint. Discussion started: 24 June 2024


Natural Hazards and Earth System Sciences
Discussions

In the forward prediction the models MRC_slow and REG_mean performed best, as they describe a mean recession behavior. The MRC_slow represents a slower recession behavior and performed slightly better. The MRC_p model represents a rather fast and the SDSC model a very slowly draining catchment state. Those occur more seldomly and hence, the related models might less often suit for low flow prediction. The REG_q05 model might be strongly affected by biases and thus may not accurately represent a realistic drainage behavior. Accordingly, for operational low flow prediction several models should be considered. In this context, by performing a backwards prediction, the best model(s) representing the current recession behavior can be chosen. This allows to change the recession model(s) for low flow prediction in every timestep and accounts for considering changes of aquifer contributions or evapotranspiration rates. It is also possible to do predictions with a model ensemble, giving a range of uncertainties, if several models perform similarly well. The described data-driven approach is, hence, very promising if the goal is to improve the predictions of low flows in gauged catchments.

https://doi.org/10.5194/nhess-2024-78
Preprint. Discussion started: 24 June 2024

Natural Hazards and Earth System Sciences
Discussions

Table A1: Catchment properties (area, station height, discharge regime) and discharge quantiles used (Q99, Q95, Q80, Q75, Q74, Q68) for the 33 catchments, calculated for the time span from 1991 to 2020.

stream	area [km^2]	station height [m a.s.l.]	discharge regime	Q99	Q95	Q80	Q75	Q74	Q68
Aabach - Moenchaltdorf	44.23	440	pluvial inférieure	0.11	0.17	0.30	0.34	0.35	0.40
Aach - Salmsach	47.38	408	pluvial inférieure	0.08	0.11	0.19	0.22	0.22	0.26
Altbach - Bassersdorf	11.77	470	pluvial inférieure	0.02	0.03	0.06	0.07	0.08	0.09
Biber - Biberbrugg	31.91	828	nivo-pluvial préalpine	0.09	0.14	0.24	0.28	0.29	0.34
Broye - Payerne	418.17	446	pluvial jurassien	0.80	1.23	2.26	2.53	2.59	2.98
Buenz - Muri	16.03	449	pluvial inférieure	0.03	0.05	0.09	0.10	0.10	0.11
Eulach - Raeterschen	31.22	470	pluvial inférieure	0.05	0.09	0.17	0.19	0.20	0.22
Glatt - Herisau	16.72	679	pluvial supérieure	0.11	0.14	0.20	0.22	0.22	0.24
Haselbach - Mettmenstetten	8.51	453	pluvial inférieure	0.01	0.02	0.04	0.05	0.05	0.05
Holzbach - Villmergen	23.92	418	pluvial inférieure	0.04	0.07	0.13	0.15	0.15	0.17
Jona - Pilgersteg	24.35	560	pluvial supérieure	0.13	0.19	0.29	0.32	0.33	0.37
Jonen - Zwillikon	37.45	460	pluvial inférieure	0.07	0.11	0.21	0.24	0.24	0.28
Kempt - Illnau	39.25	500	pluvial inférieure	0.11	0.15	0.25	0.28	0.29	0.32
Kuentenerbach - Kuenten	4.5	381	pluvial inférieure	0.01	0.01	0.02	0.02	0.02	0.03
Langete - Huttwil	59.92	602	pluvial supérieure	0.40	0.50	0.70	0.74	0.75	0.80
Luthern - Nebikon	104.68	489	pluvial supérieure	0.30	0.37	0.59	0.65	0.66	0.73
Mentue - Yvonand	105.3	448	pluvial jurassien	0.18	0.25	0.48	0.57	0.58	0.67
Murg - Waengi	80.13	469	pluvial supérieure	0.28	0.41	0.63	0.71	0.72	0.82
Pfaffnern - Vordemwald	39.06	417	pluvial inférieure	0.18	0.23	0.33	0.35	0.36	0.39
Rappengraben - Wasen_Riedbad	0.61	998	nivo-pluvial préalpine	0.00	0.00	0.00	0.01	0.01	0.01
Rietholzbach - Mosnang_Rietholz	3.19	685	pluvial supérieure	0.00	0.01	0.02	0.03	0.03	0.03
Ruederchen - Schoeftland	19.17	463	pluvial inférieure	0.05	0.07	0.11	0.12	0.12	0.14
Sellenbodenbach - Neuenkirch	10.4	519	pluvial supérieure	0.01	0.02	0.05	0.06	0.06	0.07
Sinserbach - Sins	16.25	415	pluvial inférieure	0.02	0.03	0.08	0.09	0.10	0.11
Sperbelgraben - Kurzeneialp	0.56	913	nivo-pluvial préalpine	0.00	0.00	0.00	0.01	0.01	0.01
Taegerbach - Wislikofen	13.94	390	pluvial inférieure	0.05	0.07	0.09	0.10	0.10	0.11
Uerke - Holziken	24.99	438	pluvial inférieure	0.19	0.23	0.28	0.30	0.30	0.32
Venoge - Ecublens	227.61	384	nivo-pluvial jurassien	0.36	0.50	0.94	1.11	1.14	1.36
Veveyse - Vevey	64.45	399	nivo-pluvial préalpine	0.17	0.28	0.49	0.56	0.58	0.67
Wildbach - Wetzikon	19.44	520	pluvial supérieure	0.06	0.09	0.15	0.17	0.17	0.20
Wissenbach - Boswil	11.18	460	pluvial inférieure	0.02	0.03	0.06	0.06	0.06	0.07
Wissenbach - Merenschwand	9.98	392	pluvial inférieure	0.02	0.03	0.06	0.07	0.07	0.08
Worble - Ittigen	67.04	521	pluvial inférieure	0.34	0.43	0.58	0.63	0.63	0.69

615

https://doi.org/10.5194/nhess-2024-78
Preprint. Discussion started: 24 June 2024

Natural Hazards and Earth System Sciences
Discussions

Table A2: Recession durations (D) between Q80 and Q99 for the five RAMs for the 33 investigated catchments. D declines for 30 of the 33 catchments in the following order: REG_q05 < SDSC < MRC_slow < REG_mean < MRC_p (see std. order).

stream	recession duration [d]					
	REG_q05	SDSC	MRC_slow	REG_mean	MRC_p	std. order
Aabach - Moenchaltdorf	88	42	27	17	14	yes
Aach - Salmsach	116	39	26	17	13	yes
Altbach - Bassersdorf	97	54	36	23	20	yes
Biber - Biberbrugg	62	33	22	15	14	yes
Broye - Payerne	125	68	30	19	14	yes
Buenz - Muri	109	39	34	18	17	yes
Eulach - Raeterschen	118	52	45	24	19	yes
Glatt - Herisau	76	27	29	13	10	no
Haselbach - Mettmenstetten	122	42	37	18	13	yes
Holzbach - Villmergen	157	76	44	31	23	yes
Jona - Pilgersteg	107	28	25	18	14	yes
Jonen - Zwillikon	126	56	32	21	16	yes
Kempt - Illnau	151	52	32	19	14	yes
Kuentenerbach - Kuenten	123	52	40	22	18	yes
Langete - Huttwil	130	63	45	22	15	yes
Luthern - Nebikon	99	43	33	18	13	yes
Mentue - Yvonand	156	56	37	24	15	yes
Murg - Waengi	199	58	31	21	15	yes
Pfaffnern - Vordemwald	133	72	52	26	23	yes
Rappengraben - Wasen_Riedbad	35	30	18	12	12	(yes)
Rietholzbach - Mosnang_Rietholz	79	37	27	19	16	yes
Ruederchen - Schoeftland	101	48	38	20	17	yes
Sellenbodenbach - Neuenkirch	102	67	36	17	18	yes
Sinserbach - Sins	116	47	36	20	20	(yes)
Sperbelgraben - Kurzeneialp	34	48	26	16	18	no
Taegerbach - Wislikofen	138	93	52	25	19	yes
Uerke - Holziken	152	65	58	24	15	yes
Venoge - Ecublens	140	65	33	23	15	yes
Veveyse - Vevey	116	49	28	20	14	yes
Wildbach - Wetzikon	79	31	24	15	12	yes
Wissenbach - Boswil	115	61	39	18	15	yes
Wissenbach - Merenschwand	118	55	41	22	17	yes
Worble - Ittigen	228	38	40	25	16	no

620

https://doi.org/10.5194/nhess-2024-78
Preprint. Discussion started: 24 June 2024

Natural Hazards and Earth System Sciences
Discussions

Table A3: Recession volumes (V) between Q80 and Q99 for the five RAMs for the 33 investigated catchments. V declines for 30 of the 33 catchments in the following order: REG_q05 < SDSC < MRC_slow < REG_mean < MRC_p (see std. order).

stream	recession volume [mm]					
	REG_q05	SDSC	MRC_slow	REG_mean	MRC_p	std. order
Aabach - Moenchaltdorf	30.9	16.3	10.1	6.4	5.4	yes
Aach - Salmsach	26.9	9.7	6.4	4.1	3.3	yes
Altbach - Bassersdorf	26.9	16.6	10.3	6.6	5.8	yes
Biber - Biberbrugg	24.9	14.5	9.7	6.5	6.4	yes
Broye - Payerne	37.9	20.6	9.0	5.9	4.3	yes
Buenz - Muri	34.2	13.2	10.5	5.8	5.4	yes
Eulach - Raeterschen	35.3	16.3	12.9	7.1	5.6	yes
Glatt - Herisau	58.6	22.9	23.4	10.7	8.5	no
Haselbach - Mettmenstetten	28.7	11.0	8.5	4.6	3.1	yes
Holzbach - Villmergen	45.0	23.1	12.2	8.8	6.5	yes
Jona - Pilgersteg	73.2	22.0	18.6	13.1	10.6	yes
Jonen - Zwillikon	37.2	16.2	9.6	6.3	4.9	yes
Kempt - Illnau	56.3	21.0	12.7	7.7	5.8	yes
Kuentenerbach - Kuenten	33.0	14.3	10.1	5.7	4.6	yes
Langete - Huttwil	100.0	51.5	35.2	17.6	12.1	yes
Luthern - Nebikon	34.8	16.3	11.9	6.6	4.9	yes
Mentue - Yvonand	39.5	15.0	9.5	6.2	4.0	yes
Murg - Waengi	85.3	27.8	15.0	9.9	7.4	yes
Pfaffnern - Vordemwald	72.5	41.0	28.7	14.5	12.9	yes
Rappengraben - Wasen_Riedbad	14.0	10.8	6.2	4.3	4.3	(yes)
Rietholzbach - Mosnang_Rietholz	22.0	12.0	8.5	5.9	5.2	yes
Ruederchen - Schoeftland	34.6	16.7	13.0	6.9	6.0	yes
Sellenbodenbach - Neuenkirch	22.8	15.4	7.4	4.1	3.8	yes
Sinserbach - Sins	24.0	11.6	8.2	4.6	4.6	(yes)
Sperbelgraben - Kurzeneialp	15.7	21.0	10.8	6.9	7.6	no
Taegerbach - Wislikofen	62.0	42.1	23.6	11.5	8.9	yes
Uerke - Holziken	120.6	54.0	47.9	20.0	13.0	yes
Venoge - Ecublens	30.3	15.6	7.8	5.3	3.7	yes
Veveyse - Vevey	42.9	21.4	11.7	7.9	5.9	yes
Wildbach - Wetzikon	34.8	14.2	10.7	6.6	5.5	yes
Wissenbach - Boswil	30.9	15.5	9.9	4.9	3.9	yes
Wissenbach - Merenschwand	35.3	18.3	12.4	6.8	5.3	yes
Worble - Ittigen	128.4	23.5	23.8	14.9	9.7	no

https://doi.org/10.5194/nhess-2024-78
Preprint. Discussion started: 24 June 2024

Natural Hazards and Earth System Sciences
Discussions

Table A4: Output (estimate, standard error, t-value, p-value and significance level) of the linear model comparison between the segment length and the predictable time in the forward prediction.

	estimate	std. error	t-value	p-value	significance level
intercept	-1.654	0.305	-5.424	7.16e-08	***
days	0.834	0.033	25.125	< 2.00e-16	***
modelREG_q05	0.397	0.456	0.871	0.384	
modelMRC_p	0.347	0.447	0.777	0.437	
modelMRC_slow	-0.039	0.432	-0.091	0.928	
modelSDSC	0.130	0.443	0.293	0.769	
days:modelREG_q05	-0.108	0.049	-2.209	0.027	*
days:modelMRC_p	-0.039	0.048	-0.804	0.422	
days:modelMRC_slow	-0.014	0.047	-0.293	0.770	
days:modelSDSC	-0.063	0.048	-1.311	0.190	

Table A5: Output (estimate, standard error, t-value, p-value and significance level) of the linear model comparison between the segment length and the match time in the backward prediction.

	estimate	std. error	t-value	p-value	significance level
intercept	2.203	0.328	6.710	3.02e-11	***
days	0.215	0.037	5.884	5.21e-09	***
modelREG_q05	-0.535	0.490	-1.093	0.275	
modelMRC_p	0.738	0.467	1.581	0.114	
modelMRC_slow	-1.453	0.469	-3.095	0.002	**
modelSDSC	-1.214	0.473	-2.568	0.010	*
days:modelREG_q05	0.001	0.054	0.024	0.981	
days:modelMRC_p	-0.153	0.053	-2.905	0.004	**
days:modelMRC_slow	0.250	0.052	4.809	1.72e-06	***
days:modelSDSC	0.168	0.052	3.207	0.001	**

https://doi.org/10.5194/nhess-2024-78
Preprint. Discussion started: 24 June 2024

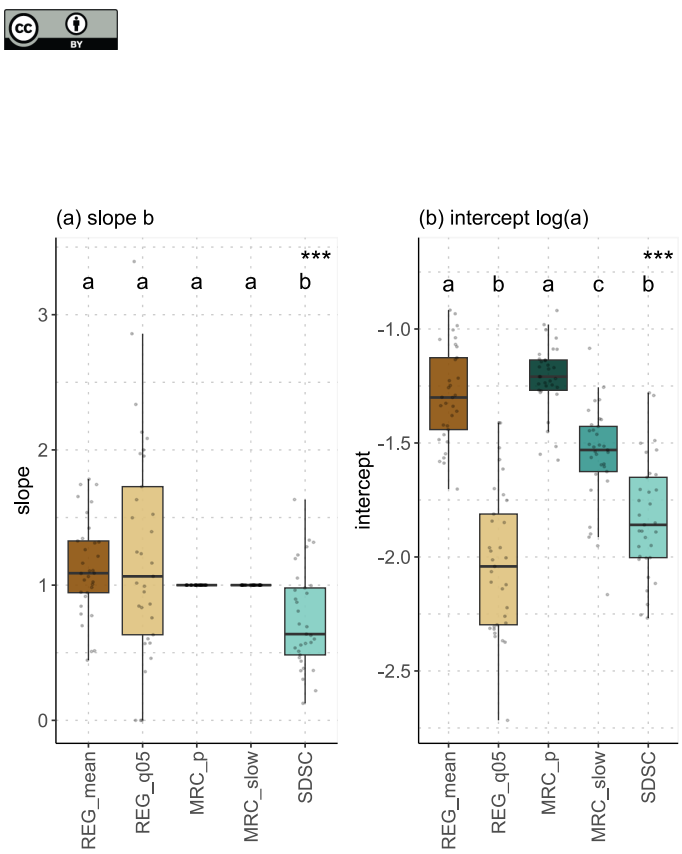

Figure A1: Comparison of the (a) slope b and the (b) intercept log(a) of the five linear regression models in the recession plot space using boxplots. The interquartile range (IQR; meaning the box) contains values between the 25 % and 75 % percentile, whereas the line within the box represents the median. The whiskers expand to a maximum of 1.5 times the IQR. The dots represent the actual values. Different letters denote significant differences among the models, equal letters denote no such difference. The three stars in the top right corner indicate the significance level overall (p-value < 0.001). The values for the SDSC are interpolated (linear regression through values of the horizontal lines).

Data & code availability

The model code for the MRC_slow and SDSC are made available once the review process is finished on envidat.ch with a persistent DOI. The discharge data used in this study belongs to the Federal Office for the Environment (FOEN) and the Cantons Zürich and Aargau, the precipitation data to MeteoSwiss. Upon request it can be ordered from those institutions. The data of the FOEN and MeteoSwiss are also openly available from 1981 to 2020 in the CAMELS-CH dataset (Höge et al., 2023a, b).

Author contribution

MM and MZ came up with the idea. Together with DHP and FL the research goals were defined. FL, MZ and DHP wrote the code of the recession segment selection. DHP applied the REG_mean, REG_q05 and MRC_p models, FL and DHP developed

650 the MRC_slow model and wrote the code. MM developed and wrote the code of the SDSC model. The analysis was done by FL and DHP, the figures by FL. MZ did the assessment of the prediction skills. MM and FL wrote the major parts of the manuscript. MZ, DHP and FS reviewed and edited the draft.

Competing interests

The authors declare that they have no conflict of interest.

655 ## Financial support

This research was funded by the Federal Office for the Environment (FOEN: 19.0081.PJ / S385-1415) and by the Canton Graubünden (ANU I DV 1680).

References

Aksoy, H. and Wittenberg, H.: Nonlinear baseflow recession analysis in watersheds with intermittent streamflow, Hydrol. Sci.
660 J., 56, 226–237, https://doi.org/10.1080/02626667.2011.553614, 2011.

Ambroise, B.: Variable water-saturated areas and streamflow generation in the small Ringelbach catchment (Vosges Mountains, France): the master recession curve as an equilibrium curve for interactions between atmosphere, surface and ground waters: Saturated Areas and Streamflow Generation in the Ringelbach Catchment, Hydrol. Process., 30, 3560–3577, https://doi.org/10.1002/hyp.10947, 2016.

665 Bart, R. and Hope, A.: Inter-seasonal variability in baseflow recession rates: The role of aquifer antecedent storage in central California watersheds, J. Hydrol., 519, 205–213, https://doi.org/10.1016/j.jhydrol.2014.07.020, 2014.

Beran, M. A. and Gustard, A.: A study into the low-flow characteristics of British rivers, J. Hydrol., 35, 147–157, https://doi.org/10.1016/0022-1694(77)90083-X, 1977.

Brunner, M. I. and Tallaksen, L. M.: Proneness of European Catchments to Multiyear Streamflow Droughts, Water Resour.
670 Res., 55, 8881–8894, https://doi.org/10.1029/2019WR025903, 2019.

Brunner, M. I., Liechti, K., and Zappa, M.: Extremeness of recent drought events in Switzerland: dependence on variable and return period choice, Nat. Hazards Earth Syst. Sci., 19, 2311–2323, https://doi.org/10.5194/nhess-19-2311-2019, 2019a.

Brunner, M. I., Farinotti, D., Zekollari, H., Huss, M., and Zappa, M.: Future shifts in extreme flow regimes in Alpine regions, Hydrol. Earth Syst. Sci., 23, 4471–4489, https://doi.org/10.5194/hess-23-4471-2019, 2019b.

675 Brunner, M. I., Björnsen Gurung, A., Zappa, M., Zekollari, H., Farinotti, D., and Stähli, M.: Present and future water scarcity in Switzerland: Potential for alleviation through reservoirs and lakes, Sci. Total Environ., 666, 1033–1047, https://doi.org/10.1016/j.scitotenv.2019.02.169, 2019c.

https://doi.org/10.5194/nhess-2024-78
Preprint. Discussion started: 24 June 2024

Brutsaert, W. and Nieber, J. L.: Regionalized drought flow hydrographs from a mature glaciated plateau, Water Resour. Res., 13, 637–643, https://doi.org/10.1029/WR013i003p00637, 1977.

Büntgen, U., Urban, O., Krusic, P. J., Rybníček, M., Kolář, T., Kyncl, T., Ač, A., Koňasová, E., Čáslavský, J., Esper, J., Wagner, S., Saurer, M., Tegel, W., Dobrovolný, P., Cherubini, P., Reinig, F., and Trnka, M.: Recent European drought extremes beyond Common Era background variability, Nat. Geosci., 14, 190–196, https://doi.org/10.1038/s41561-021-00698-0, 2021.

Byrd, R. H., Lu, P., Nocedal, J., and Zhu, C.: A Limited Memory Algorithm for Bound Constrained Optimization, SIAM J. Sci. Comput., 16, 1190–1208, https://doi.org/10.1137/0916069, 1995.

Carlier, C., Wirth, S. B., Cochand, F., Hunkeler, D., and Brunner, P.: Geology controls streamflow dynamics, J. Hydrol., 566, 756–769, https://doi.org/10.1016/j.jhydrol.2018.08.069, 2018.

Carlotto, T. and Chaffe, P. L. B.: Master Recession Curve Parameterization Tool (MRCPtool): Different approaches to recession curve analysis, Comput. Geosci., 132, 1–8, https://doi.org/10.1016/j.cageo.2019.06.016, 2019.

CH2018: CH2018 - Climate Scenarios for Switzerland, National Centre for Climate Services, Zurich, 2018.

Chen, X., Zhang, Y., Xue, X., Zhang, Z., and Wei, L.: Estimation of baseflow recession constants and effective hydraulic parameters in the karst basins of southwest China, Hydrol. Res., 43, 102–112, https://doi.org/10.2166/nh.2011.136, 2012.

Coutagne, A.: 2 ME Partie Les Variations de Débit en Période Non Influencée par les Précipitations - le Débit D'infiltration (Corrélations Fluviales Internes), Houille Blanche, 34, 416–436, https://doi.org/10.1051/lhb/1948053, 1948.

Coxon, G., Freer, J., Westerberg, I. K., Wagener, T., Woods, R., and Smith, P. J.: A novel framework for discharge uncertainty quantification applied to 500 UK gauging stations, Water Resour. Res., 51, 5531–5546, https://doi.org/10.1002/2014WR016532, 2015.

Dralle, D. N., Karst, N. J., Charalampous, K., Veenstra, A., and Thompson, S. E.: Event-scale power law recession analysis: quantifying methodological uncertainty, Hydrol. Earth Syst. Sci., 21, 65–81, https://doi.org/10.5194/hess-21-65-2017, 2017.

Dunn, O. J.: Multiple Comparisons Using Rank Sums, Technometrics, 6, 241–252, https://doi.org/10.1080/00401706.1964.10490181, 1964.

Eng, K., Wolock, D. M., and Wieczorek, M.: Predicting baseflow recession characteristics at ungauged stream locations using a physical and machine learning approach, Adv. Water Resour., 175, 104440, https://doi.org/10.1016/j.advwatres.2023.104440, 2023.

Federer, C. A.: Forest transpiration greatly speeds streamflow recession, Water Resour. Res., 9, 1599–1604, https://doi.org/10.1029/WR009i006p01599, 1973.

Fink, A. H., Brücher, T., Krüger, A., Leckebusch, G. C., Pinto, J. G., and Ulbrich, U.: The 2003 European summer heatwaves and drought -synoptic diagnosis and impacts: European heatwave - impacts, Weather, 59, 209–216, https://doi.org/10.1256/wea.73.04, 2004.

Fiorotto, V. and Caroni, E.: A new approach to master recession curve analysis, Hydrol. Sci. J., 58, 966–975, https://doi.org/10.1080/02626667.2013.788248, 2013.

Floriancic, M. G., Spies, D., Van Meerveld, I. H. J., and Molnar, P.: A multi-scale study of the dominant catchment characteristics impacting low-flow metrics, Hydrol. Process., 36, e14462, https://doi.org/10.1002/hyp.14462, 2022.

FOEN: Effects of climate change on Swiss water bodies, Federal Office for the Environment FOEN, Bern, 2021.

FOEN: Personal communication about the use of rating curves for the calculation of discharge time series of FOEN gauging stations, 2024.

Freire-González, J., Decker, C., and Hall, J. W.: The Economic Impacts of Droughts: A Framework for Analysis, Ecol. Econ., 132, 196–204, https://doi.org/10.1016/j.ecolecon.2016.11.005, 2017.

Friedman, M.: The Use of Ranks to Avoid the Assumption of Normality Implicit in the Analysis of Variance, J. Am. Stat. Assoc., 32, 675–701, https://doi.org/10.1080/01621459.1937.10503522, 1937.

Gao, M., Chen, X., Singh, S. K., and Wei, L.: An improved method to estimate the rate of change of streamflow recession and basin synthetic recession parameters from hydrographs, J. Hydrol., 604, 127254, https://doi.org/10.1016/j.jhydrol.2021.127254, 2022.

Gnann, S. J., McMillan, H. K., Woods, R. A., and Howden, N. J. K.: Including Regional Knowledge Improves Baseflow Signature Predictions in Large Sample Hydrology, Water Resour. Res., 57, e2020WR028354, https://doi.org/10.1029/2020WR028354, 2021.

Gottschalk, L., Tallaksen, L. M., and Perzyna, G.: Derivation of low flow distribution functions using recession curves, J. Hydrol., 194, 239–262, https://doi.org/10.1016/S0022-1694(96)03214-3, 1997.

Griffiths, G. A. and McKerchar, A. I.: Comparison of a deterministic and a statistical model for predicting streamflow recession curves, J. Hydrol. N. Z., 54, 53–62, 2015.

Hall, F. R.: Base-Flow Recessions-A Review, Water Resour. Res., 4, 973–983, https://doi.org/10.1029/WR004i005p00973, 1968.

Hanel, M., Rakovec, O., Markonis, Y., Máca, P., Samaniego, L., Kyselý, J., and Kumar, R.: Revisiting the recent European droughts from a long-term perspective, Sci. Rep., 8, 9499, https://doi.org/10.1038/s41598-018-27464-4, 2018.

Höge, M., Kauzlaric, M., Siber, R., Schönenberger, U., Horton, P., Schwanbeck, J., Floriancic, M. G., Viviroli, D., Wilhelm, S., Sikorska-Senoner, A. E., Addor, N., Brunner, M., Pool, S., Zappa, M., and Fenicia, F.: CAMELS-CH: hydro-meteorological time series and landscape attributes for 331 catchments in hydrologic Switzerland, Earth Syst. Sci. Data, 15, 5755–5784, https://doi.org/10.5194/essd-15-5755-2023, 2023a.

Höge, M., Kauzlaric, M., Siber, R., Schönenberger, U., Horton, P., Schwanbeck, J., Floriancic, M. G., Viviroli, D., Wilhelm, S., Sikorska-Senoner, A. E., Addor, N., Brunner, M., Pool, S., Zappa, M., and Fenicia, F.: Catchment attributes and hydro-meteorological time series for large-sample studies across hydrologic Switzerland (CAMELS-CH) (0.8), https://doi.org/10.5281/ZENODO.7784632, 2023b.

IPCC: Climate Change 2023: Synthesis Report. Contribution of Working Groups I, II and III to the Sixth Assessment Report of the Intergovernmental Panel on Climate Change [Core Writing Team, H. Lee and J. Romero (eds.)], Intergovernmental Panel on Climate Change (IPCC), Geneva, Switzerland, https://doi.org/10.59327/IPCC/AR6-9789291691647, 2023.

Jachens, E. R., Rupp, D. E., Roques, C., and Selker, J. S.: Recession analysis revisited: impacts of climate on parameter estimation, Hydrol. Earth Syst. Sci., 24, 1159–1170, https://doi.org/10.5194/hess-24-1159-2020, 2020.

James, L. D. and Thompson, W. O.: Least Squares Estimation of Constants in a Linear Recession Model, Water Resour. Res., 6, 1062–1069, https://doi.org/10.1029/WR006i004p01062, 1970.

Karlsen, R. H., Seibert, J., Grabs, T., Laudon, H., Blomkvist, P., and Bishop, K.: The assumption of uniform specific discharge: unsafe at any time?, Hydrol. Process., 30, 3978–3988, https://doi.org/10.1002/hyp.10877, 2016.

Kirchner, J. W.: Catchments as simple dynamical systems: Catchment characterization, rainfall-runoff modeling, and doing hydrology backward: CATCHMENTS AS SIMPLE DYNAMICAL SYSTEMS, Water Resour. Res., 45, https://doi.org/10.1029/2008WR006912, 2009.

Knisel, W. G.: Baseflow recession analysis for comparison of drainage basins and geology, J. Geophys. Res., 68, 3649–3653, https://doi.org/10.1029/JZ068i012p03649, 1963.

Krakauer, N. Y. and Temimi, M.: Stream recession curves and storage variability in small watersheds, Hydrol. Earth Syst. Sci., 15, 2377–2389, https://doi.org/10.5194/hess-15-2377-2011, 2011.

Laaha, G. and Blöschl, G.: Seasonality indices for regionalizing low flows, Hydrol. Process., 20, 3851–3878, https://doi.org/10.1002/hyp.6161, 2006.

Laaha, G., Gauster, T., Tallaksen, L. M., Vidal, J.-P., Stahl, K., Prudhomme, C., Heudorfer, B., Vlnas, R., Ionita, M., Van Lanen, H. A. J., Adler, M.-J., Caillouet, L., Delus, C., Fendekova, M., Gailliez, S., Hannaford, J., Kingston, D., Van Loon, A. F., Mediero, L., Osuch, M., Romanowicz, R., Sauquet, E., Stagge, J. H., and Wong, W. K.: The European 2015 drought from a hydrological perspective, Hydrol. Earth Syst. Sci., 21, 3001–3024, https://doi.org/10.5194/hess-21-3001-2017, 2017.

Lamb, R. and Beven, K.: Using interactive recession curve analysis to specify a general catchment storage model, Hydrol. Earth Syst. Sci., 1, 101–113, https://doi.org/10.5194/hess-1-101-1997, 1997.

Langbein, W. B.: Some channel-storage studies and their application to the determination of infiltration, Trans. Am. Geophys. Union, 19, 435, https://doi.org/10.1029/TR019i001p00435, 1938.

Lustenberger, F., Liechti, K., Barben, M., and Zappa, M.: Wasserhaushalt der Schweiz 2021. Einordnung und Besonderheiten, Einführung der Normperiode 1991 bis 2020, Wasser, Energie, Luft, 114, 94–97, https://www.dora.lib4ri.ch/wsl/islandora/object/wsl:30683, 2022.

Lustenberger, F., Zappa, M., Liechti, K., and Barben, M.: Wasserhaushalt der Schweiz 2022. Einordnung und Besonderheiten, Wasser, Energie, Luft, 2, 80–83, https://www.dora.lib4ri.ch/wsl/islandora/object/wsl:33506, 2023.

Maillet, E.: Essais d'Hydraulique souterraine et fluviale, Nature, 72, 25–26, https://doi.org/10.1038/072025a0, 1905.

Makridakis, S.: Accuracy measures: theoretical and practical concerns, Int. J. Forecast., 9, 527–529, https://doi.org/10.1016/0169-2070(93)90079-3, 1993.

Mendoza, G. F., Steenhuis, T. S., Walter, M. T., and Parlange, J.-Y.: Estimating basin-wide hydraulic parameters of a semi-arid mountainous watershed by recession-flow analysis, J. Hydrol., 279, 57–69, https://doi.org/10.1016/S0022-1694(03)00174-4, 2003.

MeteoSwiss: Documentation of MeteoSwiss Grid-Data Products - Daily Precipitation (final analysis): RhiresD, 2021.

Meusburger, K., Trotsiuk, V., Schmidt-Walter, P., Baltensweiler, A., Brun, P., Bernhard, F., Gharun, M., Habel, R., Hagedorn, F., Köchli, R., Psomas, A., Puhlmann, H., Thimonier, A., Waldner, P., Zimmermann, S., and Walthert, L.: Soil–plant

interactions modulated water availability of Swiss forests during the 2015 and 2018 droughts, Glob. Change Biol., 28, 5928–5944, https://doi.org/10.1111/gcb.16332, 2022.

Muelchi, R., Rössler, O., Schwanbeck, J., Weingartner, R., and Martius, O.: River runoff in Switzerland in a changing climate – changes in moderate extremes and their seasonality, Hydrol. Earth Syst. Sci., 25, 3577–3594, https://doi.org/10.5194/hess-25-3577-2021, 2021a.

Muelchi, R., Rössler, O., Schwanbeck, J., Weingartner, R., and Martius, O.: River runoff in Switzerland in a changing climate – runoff regime changes and their time of emergence, Hydrol. Earth Syst. Sci., 25, 3071–3086, https://doi.org/10.5194/hess-25-3071-2021, 2021b.

Nathan, R. J. and McMahon, T. A.: Evaluation of automated techniques for base flow and recession analyses, Water Resour. Res., 26, 1465–1473, https://doi.org/10.1029/WR026i007p01465, 1990.

Nurkholis, A., Adji, T. N., Haryono, E., Cahyadi, A., and Suprayogi, S.: Time series analysis applications for karst aquifer characterisation in Pindul Cave karst system, Indonesia, Acta Carsologica, 48, https://doi.org/10.3986/ac.v48i1.6745, 2019.

O'Brien, R. J., Misstear, B. D., Gill, L. W., Deakin, J. L., and Flynn, R.: Developing an integrated hydrograph separation and lumped modelling approach to quantifying hydrological pathways in Irish river catchments, J. Hydrol., 486, 259–270, https://doi.org/10.1016/j.jhydrol.2013.01.034, 2013.

Posavec, K., Bacani, A., and Nakic, Z.: A Visual Basic Spreadsheet Macro for Recession Curve Analysis, Ground Water, 0, 060526082055001-???, https://doi.org/10.1111/j.1745-6584.2006.00226.x, 2006.

Posavec, K., Parlov, J., and Nakić, Z.: Fully Automated Objective-Based Method for Master Recession Curve Separation, Ground Water, 48, 598–603, https://doi.org/10.1111/j.1745-6584.2009.00669.x, 2010.

Posavec, K., Giacopetti, M., Materazzi, M., and Birk, S.: Method and Excel VBA Algorithm for Modeling Master Recession Curve Using Trigonometry Approach, Groundwater, 55, 891–898, https://doi.org/10.1111/gwat.12549, 2017.

Pushpalatha, R., Perrin, C., Moine, N. L., and Andréassian, V.: A review of efficiency criteria suitable for evaluating low-flow simulations, J. Hydrol., 420–421, 171–182, https://doi.org/10.1016/j.jhydrol.2011.11.055, 2012.

Reddyvaraprasad, C., Patnaik, S., and Biswal, B.: Recession flow prediction in gauged and ungauged basins by just considering past discharge information, Hydrol. Sci. J., 65, 21–32, https://doi.org/10.1080/02626667.2019.1643465, 2020.

Rivera-Ramirez, H. D., Warner, G. S., and Scatena, F. N.: PREDICTION OF MASTER RECESSION CURVES AND BASEFLOW RECESSIONS IN THE LUQUILLO MOUNTAINS OF PUERTO RICO, J. Am. Water Resour. Assoc., 38, 693–704, https://doi.org/10.1111/j.1752-1688.2002.tb00990.x, 2002.

Roques, C., Rupp, D. E., and Selker, J. S.: Improved streamflow recession parameter estimation with attention to calculation of − dQ/dt, Adv. Water Resour., 108, 29–43, https://doi.org/10.1016/j.advwatres.2017.07.013, 2017.

Rupp, D. E. and Selker, J. S.: On the use of the Boussinesq equation for interpreting recession hydrographs from sloping aquifers, Water Resour. Res., 42, 2006WR005080, https://doi.org/10.1029/2006WR005080, 2006.

Santos, A. C., Portela, M. M., Rinaldo, A., and Schaefli, B.: Estimation of streamflow recession parameters: New insights from an analytic streamflow distribution model, Hydrol. Process., 33, 1595–1609, https://doi.org/10.1002/hyp.13425, 2019.

Seneviratne, S. I., Lehner, I., Gurtz, J., Teuling, A. J., Lang, H., Moser, U., Grebner, D., Menzel, L., Schroff, K., Vitvar, T., and Zappa, M.: Swiss prealpine Rietholzbach research catchment and lysimeter: 32 year time series and 2003 drought event, Water Resour. Res., 48, 2011WR011749, https://doi.org/10.1029/2011WR011749, 2012.

Shaw, S. B., McHardy, T. M., and Riha, S. J.: Evaluating the influence of watershed moisture storage on variations in base flow recession rates during prolonged rain-free periods in medium-sized catchments in New York and Illinois, USA: Control of Moisture Storage on Base Flow Recession Rates, Water Resour. Res., 49, 6022–6028, https://doi.org/10.1002/wrcr.20507, 2013.

Singh, S. K. and Griffiths, G. A.: Prediction of Streamflow Recession Curves in Gauged and Ungauged Basins, Water Resour. Res., 57, e2021WR030618, https://doi.org/10.1029/2021WR030618, 2021.

Smakhtin, V. U.: Low flow hydrology: a review, J. Hydrol., 240, 147–186, https://doi.org/10.1016/S0022-1694(00)00340-1, 2001.

Snyder, F. F.: A conception of runoff-phenomena, Trans. Am. Geophys. Union, 20, 725, https://doi.org/10.1029/TR020i004p00725, 1939.

Stahl, K., Vidal, J.-P., Hannaford, J., Tijdeman, E., Laaha, G., Gauster, T., and Tallaksen, L. M.: The challenges of hydrological drought definition, quantification and communication: an interdisciplinary perspective, Proc. Int. Assoc. Hydrol. Sci., 383, 291–295, https://doi.org/10.5194/piahs-383-291-2020, 2020.

Staudinger, M., Stahl, K., Seibert, J., Clark, M. P., and Tallaksen, L. M.: Comparison of hydrological model structures based on recession and low flow simulations, Hydrol. Earth Syst. Sci., 15, 3447–3459, https://doi.org/10.5194/hess-15-3447-2011, 2011.

Stoelzle, M., Stahl, K., and Weiler, M.: Are streamflow recession characteristics really characteristic?, Hydrol. Earth Syst. Sci., 17, 817–828, https://doi.org/10.5194/hess-17-817-2013, 2013.

Stoelzle, M., Stahl, K., Morhard, A., and Weiler, M.: Streamflow sensitivity to drought scenarios in catchments with different geology, Geophys. Res. Lett., 41, 6174–6183, https://doi.org/10.1002/2014GL061344, 2014.

Stoelzle, M., Schuetz, T., Weiler, M., Stahl, K., and Tallaksen, L. M.: Beyond binary baseflow separation: a delayed-flow index for multiple streamflow contributions, Hydrol. Earth Syst. Sci., 24, 849–867, https://doi.org/10.5194/hess-24-849-2020, 2020.

Tallaksen, L. M.: A review of baseflow recession analysis, J. Hydrol., 165, 349–370, https://doi.org/10.1016/0022-1694(94)02540-R, 1995.

Teuling, A. J., Lehner, I., Kirchner, J. W., and Seneviratne, S. I.: Catchments as simple dynamical systems: Experience from a Swiss prealpine catchment, Water Resour. Res., 46, 2009WR008777, https://doi.org/10.1029/2009WR008777, 2010.

Thomas, B. F., Vogel, R. M., and Famiglietti, J. S.: Objective hydrograph baseflow recession analysis, J. Hydrol., 525, 102–112, https://doi.org/10.1016/j.jhydrol.2015.03.028, 2015.

Toebes, C., Morrissey, W. B., Shorter, R., and Hendy, M.: Base-flow-recession curves, in: Handbook of Hydrological Procedures. Proc. 8, Ministry of Works, Wellington, New Zealand, 1969.

Van Lanen, H. A. J., Laaha, G., Kingston, D. G., Gauster, T., Ionita, M., Vidal, J., Vlnas, R., Tallaksen, L. M., Stahl, K., Hannaford, J., Delus, C., Fendekova, M., Mediero, L., Prudhomme, C., Rets, E., Romanowicz, R. J., Gailliez, S., Wong, W.

https://doi.org/10.5194/nhess-2024-78
Preprint. Discussion started: 24 June 2024

K., Adler, M., Blauhut, V., Caillouet, L., Chelcea, S., Frolova, N., Gudmundsson, L., Hanel, M., Haslinger, K., Kireeva, M., Osuch, M., Sauquet, E., Stagge, J. H., and Van Loon, A. F.: Hydrology needed to manage droughts: the 2015 European case, Hydrol. Process., 30, 3097–3104, https://doi.org/10.1002/hyp.10838, 2016.

Vogel, R. M. and Kroll, C. N.: Regional geohydrologic-geomorphic relationships for the estimation of low-flow statistics, Water Resour. Res., 28, 2451–2458, https://doi.org/10.1029/92WR01007, 1992.

Wang, D. and Cai, X.: Recession slope curve analysis under human interferences, Adv. Water Resour., 33, 1053–1061, https://doi.org/10.1016/j.advwatres.2010.06.010, 2010.

Weingartner, R. and Aschwanden, H.: HADES - Tafel 5.2, in: Hydrologischer Atlas der Schweiz, FOEN (ed.). Bundesamt für Landestopographie swisstopo, Bern, 1992.

Weisman, R. N.: The effect of evapotranspiration on streamflow recession, Hydrol. Sci. Bull., 22, 371–377, https://doi.org/10.1080/02626667709491731, 1977.

Westerberg, I. K. and McMillan, H. K.: Uncertainty in hydrological signatures, Hydrol. Earth Syst. Sci., 19, 3951–3968, https://doi.org/10.5194/hess-19-3951-2015, 2015.

Wirth, S., Carlier, C., Cochand, F., Hunkeler, D., and Brunner, P.: Lithological and Tectonic Control on Groundwater Contribution to Stream Discharge During Low-Flow Conditions, Water, 12, 821, https://doi.org/10.3390/w12030821, 2020.

WMO: Manual on low-flow estimation and prediction, World Meteorological Organization, Geneva, Switzerland, 2008.

Zappa, M. and Kan, C.: Extreme heat and runoff extremes in the Swiss Alps, Nat. Hazards Earth Syst. Sci., 7, 375–389, https://doi.org/10.5194/nhess-7-375-2007, 2007.